Development of Adaptive Control for Railway Vehicles Braking System: Case study for AA-LRT

Yared Kassahun Abadi

A Thesis Submitted to

The School of Electrical and Computer Engineering

Presented in Fulfillment of the requirements for the Degree of Master of Science (Electrical Engineering for Railway Systems)

Addis Ababa University

Addis Ababa, Ethiopia

June 2017

Addis Ababa University

Addis Ababa Institute of Technology

School of Electrical and Computer Engineering

This is to certify that the thesis prepared by Yared Kassahun, entitled: *Development of Adaptive Control for Railway Vehicles Braking System: Case study for AA-LRT* and submitted in partial fulfillment of the requirements for the Degree of Master of Science (Electrical Engineering for Railway Systems) complies with the regulations of the university and meets the accepted standards with respect to originality and quality.

Signed by Examining Committee:

Examiner_____ Signature_____ Date_____

Examiner_____ Signature_____ Date_____

Advisor_____ Signature_____ Date_____

Advisor_____ Signature_____ Date_____

_____

School or Center Chair Person

Declaration

I, Yared Kassahun, declare that this thesis is my original work, has not been presented for a degree in this or other universities. All sources of materials used for this thesis work have been fully acknowledged.

Name: Yared Kassahun Signature: _____

Place: Addis Ababa University, Addis Ababa

Date of Submission: _____

This thesis has been submitted for examination with my approval as a university advisor.

Mr. Abi Abate Signature:

Advisor's Name _____

Abstract

Since railway transport is one of the main modes of land transportation, stopping rail vehicles at stations is the eventual routine of the service. The critical challenge in railway vehicles braking system is accurately limiting train braking distance under different operation conditions, since the train movement is on metal rail with low adhesion coefficient relative to road lines. Accurate estimation of the braking distance will allow trains to be spaced closer together, with reasonable confidence that they will stop without colliding each other. Therefore, a dedicated braking control system is intensely required, which can enhance fast and reliable control actions. Currently trams used in Addis Ababa Light Rail Transit equipped with Proportional and Integral controller based closed loop Variable Voltage Variable Frequency drive system. The conventional Proportional and Integral controller with fixed gain and normal feedback is unable to achieve desired braking control performance under different disturbances.

The motive of this work is to investigate the existing train braking control system and develop a new adaptive control mechanism that can handle disturbances and gives adequate control response. Model reference adaptive controller tunes a given proportional and integral controller in such a way that error between the speed command and actual speed will be minimized to improve braking control action. A well-known Massachusetts Institute of Technology (gradient) adaptation algorithm is used to develop the proposed adaptive control system. The existing and the newly developed control systems are compared using MathLab environment.

According to the simulation results for disturbance handling model reference adaptive system has 1.504 % overshoot and 1.876 rad/sec speed error which is much smaller than proportional and integral controller with 92.7 % overshoot and 6.26 rad/sec speed error. Also model reference adaptive controller significantly improved braking distance and time around 25% more than proportional and integral controller by giving fast response.

Keywords: Addis Ababa Light Rail Transit (**AA- LRT**), Proportional and Integral controller **(PI)**, Variable Voltage Variable Frequency (**VVVF**), Model Reference Adaptive Control (**MRAC)**, Massachusetts Institute of Technology (**MIT).**

Acknowledgment

I would like to give my ultimate appreciation and respect to my father Kassahun Abadi and my mother Tewabech Mamo for giving me the passion, courage and everything they have to see my success.

Accomplishment of this thesis is achieved with the commitment and dedication of my advisor Mr. Abi Abate, he understand my situations and help me in all cases to bring my thesis to reality. I would like to express my gratitude to him.

I am delighted when I thank Emebet Gebeyehu and my friends who support and encourage me unconditionally to complete my thesis.

Finally more than all I thank almighty God for everything.

Table of Contents

Declaration i
Abstract ii
Acknowledgment iii
List of Figures vi
List of Tables viii
List of Symbols and Abbreviations ix
List of Symbols ix
List of Abbreviations xii
Chapter One 1
Introduction 1
1.1 Background 1
1.2 Statement of the Problem 3
1.3 Objective of the Study 4
1.3.1 General Objective 4
1.3.2 Specific Objectives 4
1.4 Scope of the Thesis Work 5
1.5 Methodology 5
1.6 Thesis Contribution 7
1.7 Thesis Organization 7
Chapter Two 8
Theoretical Background and Literature Review 8
2.1 Theoretical Background 8
2.1.1 Train Dynamics 8
2.1.2 Railway Vehicles Braking System 12
2.1.3 Main Parts of Electrical Traction and Braking System. 14
2.1.4 Model Reference Adaptive Control 23
2.2 Literature Review 29
Chapter Three 31
Mathematical Modeling and Development of Adaptive Controller 31
3.1 Longitudinal Train Dynamics Modelling for AA-LRT 31
3.1.1 Train Resistance Forces 31
3.1.2 Braking Force 35

3.1.3 Braking Distance and Time 38
3.2 Electrical Traction and Braking System Modelling 41
3.2.1 Traction Power Converter Modelling 41
3.2.2 Traction Motor Modelling 45
3.2.3 PI Based VVVF Speed Controller 48
3.3 Modelling of PI Controlled Plant 48
3.4 Development of Model Reference Adaptive Controller 52
3.4.1 Plant Model to be Controlled 53
3.4.2 Reference Model 54
3.4.3 Adaptation Mechanism 54
Chapter Four 60
Simulation Result Analysis and Discussion 60
4.1 MathLab Simulation of Proportional and Integral Controller 61
4.1.1 Load Rejection in PI Controller 62
4.1.2 Braking Transient Response of PI Controller 63
4.1.3 Disturbance Rejection of PI Controller 64
4.2 Model Reference Adaptive Controller 65
4.2.1 Load Rejection in MRAC Controller 65
4.2.2 Braking Transient Response of MRAC Controller 66
4.2.3 Disturbance Rejection of MRAC Controller 67
4.3 Performance of PI and MRAC Controllers in AA-LRT Braking System Model 68
4.3.1 Simulation Results 70
Chapter Five 74
Conclusion and Recommendation for Future Work 74
5.1 Conclusion 74
5.2 Recommendations 75
References 76
Appendix 80

List of Figures

Figure 1.1 Flow Chart for Adopted Research Methodology 6
Figure 2.1 Grade Resistance of Moving Body [7] 11
Figure 2.2 Curve in Railway Track [7] 12
Figure 2.3 Typical Torque-Speed Curve for Induction Machine 14
Figure 2.4 Steady State per Phase Equivalent Circuit of Squirrel Cage Motor 15
Figure 2.5 Induction Motor Simplified Equivalent Circuit with Shorted Rotor 16
Figure 2.6 PWM Inverter Fed Induction Motor Drive 17
Figure 2.7 (a) Principle of Sinusoidal PWM for Three-Phase Bridge Inverter 18
Figure 2.7 (b) Line Voltage Waves of PWM Inverter 19
Figure 2.8 Torque-Speed Curves with E/f Held Constant 20
Figure 2.9 Closed Loop Speed Control of Induction Motor 21
Figure 2.10 Proportional Integral (PI) Controller 22
Figure 2.11 Block Diagram of MRAC System 24
Figure 3.1 Longitudinal Forces Acting on Railway Vehicle 31
Figure 3.2 Gradient Distribution on North-South LRT Line 33
Figure 3.3 Gradient Distribution on East-West LRT Line 33
Figure 3.4 Curve Radius between Stations in AA-LRT 34
Figure 3.5 MathLab Simulink Model for Calculating Braking Torque 37
Figure 3.6 Speed Time Curve for Urban Trams 38
Figure 3.7 Speed Time Curve for Different Deceleration Values 40
Figure 3.8 IGBT Based Voltage Source Inverter Supplied Induction Motor [34] 42
Figure 3.9 Pulse Width Modulation for Inverter Switching 42
Figure 3.10 Comparator Input, Sinusoidal and Triangular Wave 44
Figure 3.11 VVVF Inverter Gate Trigger Pulses 44
Figure 3.12 Torque Speed Characteristics of 130 KW Induction Motor 46
Figure 3.13 Modelling of Inverter Fed 130 KW Induction Motor 46
Figure 3.13 Characteristics 130 KW Induction Motor 47
Figure 3.14 Closed-Loop V/Hz Constant Control 48
Figure 3.16 MathLab Simulink Model for PI Controller 49
Figure 3.17 MathLab Simulink Model for PI Controller with Actual Data 51

Figure 3.18 Block Diagram of Model Reference Adaptive Control 52
Figure 3.19 Model Reference Adaptive Controller for AA-LRT Train Braking System 58
Figure 4.1 Load Rejection of PI Controller 62
Figure 4.2 Braking Transient Response of PI Controller 63
Figure 4.3 Disturbance Rejection of PI Controller 64
Figure 4.4 MRAC Controller Load Rejection for Different Adaptive Gain Values 65
Figure 4.5 Braking Transient Response of MRAC Controller 66
Figure 4.6 Disturbance Rejection of MRAC Controller 67
Figure 4.7 PI and MRAC Controllers in AA-LRT Braking System Compact MathLab Model .. 69
Figure 4.8 Speed Response of PI and MRAC Controllers in Braking Model. 70
Figure 4.9 Torque and Deceleration Response of PI and MRAC Controllers 71

List of Tables

Table 3.1 Brake Pattern for Different Braking Operations 36
Table 3.2 Specifications of Traction Motor 45
Table 4.1 Parameters for Simulation 60
Table 4.2 Braking Performance of PI and MRAC 72
Table 4.3 Braking Performance Improvement in MRAC 72

List of Symbols and Abbreviations

List of Symbols

R_r	Propulsion resistance (N/ton)
F_c	Curve resistance force
W	Weight of train (ton)
R	Curve radius (meter)
F_g	Gradient resistance force
r	Rolling resistance
R	Train rolling resistance
A	Rolling resistance component independent of train speed
B	Train resistance dependent on speed
C	Drag coefficient based on the shape of the front of the train and other features affecting air turbulence
V	Train speed
e	Axle load in tonne
S	Slip
ω_S	Synchronous speed (radians per second)
ω_m	Rotor mechanical speed (radians per second)
Rs	Stator winding resistance
Xls	Stator winding leakage reactance
Xm	Excitation reactance
Xlr	Rotor winding leakage reactance
Rr	Rotor winding resistance
f	frequency

fc	carrier frequency
V_P	Peak value of the modulating wave and
V_T	Peak value of the carrier wave
MI	Modulation Index
$E1$	Voltage induced in the stator
Φ	Air gap flux
P_{ag}	Total air-gap power
I_2	Rotor current referred to stator
I_s	Stator circuit current
r_s	Stator circuit winding resistance
r_s	Rotor circuit winding resistance
L_s	Stator winding inductance
L_r	Stator winding inductance
$U(s)$	Command signal
$e(s)$	Error
K_p	Proportional gain
K_i	Integral gain
$\psi(\phi)$	Cost Function
ϕ	Controller parameter vector,
γ	Adaptive gain
$\frac{\partial e}{\partial \phi}$	Sensitivity derivative.
$y(s)$	Plant output
$u_c\ (s)$	Command signal

$W_m(s)$	Actual speed of motor
$W_c\ (s)$	Speed command
J	Motor shaft inertia
B	Viscous friction torque coefficient
K_p	Proportional gain
K_i	Integral gain
$W_{model}(s)$	Speed output from the reference model
γ_p	Adaptation gain for proportional controller
γ_i	Adaptation gain for integral controller

List of Abbreviations

ERC	Ethiopian Railways Corporation
AA-LRT	Addis Ababa Light Rail Transit
PI	Proportional and Integral controller
MRAC	Model Reference Adaptive Control
AC	Alternating Current
DC	Direct Current
GTO	Gate Turn-Off Thyristor
IGBT	Insulated-Gate Bipolar Transistor
VVVF	Variable Voltage Variable Frequency
PWM	Pulse Width Modulation
MIT	Massachusetts Institute of Technology
MC	Motor Car
TC	Trailer Car
HSCB	High Speed Circuit Breaker
CSI	Current Source Inverter
VSI	Voltage Source Inverter
SPWM	Sinusoidal Pulse Width Modulation Inverter
V/Hz	Volt per Hertz

Chapter One

Introduction

1.1 Background

It is apparently known that the safety credit of any land transportation system is primarily given to braking system efficiency. Railway vehicles have a very complex braking system comparing to the remaining sectors due to the fact that the vehicle is traveling on smooth petal gage. In order to achieve the braking process, different interactions i.e. electrical, mechanical, thermal, pneumatic, are held. Therefore, it is affected by certain and uncertain factors like weather, braking coefficient dispersion, rolling stock dynamics etc[1,2].

The modern design of trains incorporating three phase induction motors and converter inverter enables recovery of a major portion of consumed electricity by way of using electrical braking which is mainly contain regenerative and resistance braking in failure of regenerative braking. Regenerative braking and resistance braking are mechanisms that decelerates the vehicle by converting its kinetic energy into electric energy. These methods have been widely applied on electric trains, particularly in metro transit systems. Compared with trains with only mechanical braking, studies show that the use of regenerative braking on metro trains can provide energy savings of 10% to 45%, depending on system characteristics [3]. But in the same cases with other braking types regenerative and resistance braking will affected by the uncertainties of random events. Modeling the longitudinal dynamics of trains is important to understand the effect of these factors while the rail vehicle is on operation. This can also help with better understanding the effects of braking forces, other forces and moments that resist the forward motion of the train. Improving dynamic braking forces will results stopping the train in shorter distance and in safe manner [4]. Thus, an adequate control system is needed to achieve this performance improvement.

Addis Ababa Light Rail Transit (AA-LRT) project is electrified light rail transit owned by Ethiopian railway corporation (ERC), which is total length of 34.25 km (North-South line 16.9 km and East-West line 17.35 km). Vehicles used in this transit are 70% low floor modern trams with maximum operating speed of 70km/h. The employed brake system incorporates modular design with simple interface to meet requirements of modern brake system. It is equipped with

electric brake (mainly regenerative brake), hydraulic disc brake and track brake, which are independent of each other. Regenerative brake should be preferably applied as service brake for vehicles. Role of regenerative brake should be utilized to a maximum extent and return energy back to power network. In case of insufficiency in regenerative braking force or failure resistance brake will be automatically put into service for compensation [5].

The existing proportional integral controller system is not reliable for applications with high dynamic character like braking system. So this paper is motivated to point out how PI controller will be affected by disturbances, how this disturbance affect the overall braking system and came up with a solution which will overcome the problems countered in PI controller by designing a model reference based adaptive controller.

1.2 Statement of the Problem

While achieving safe and effective brake actions to allow speed reductions, it is very important that brake control action and performance should not be influenced by disturbances like environmental conditions, wheel/rail interactions and variable loads. Based on the information found from AA-LRT rolling stock department, the vehicles used in the light rail transit equipped regenerative braking incorporating with other mechanical brake types under the control of proportional and integral controller plus VVVF speed drive. These train braking control system, which is based on pre-sated train (plant), and controller parameters, is not capable of learning uncertainties to guarantee safe operation to stop the train in short time. PI controller can never achieve perfect control, that is, keep the speed of the train continuously at the desired set point value and fast response in the presence of disturbance or set point changes .This paper is motivated to develop a control system which can learn (measure and change train parameters) and compensate (tune controller parameters in real time) under disturbances.

1.3 Objective of the Study

1.3.1 General Objective

The general objective of this thesis is:

- ✓ To develop efficient braking system which can give better braking action over different loading and disturbance conditions.

1.3.2 Specific Objectives

The Specific objectives of this research are stated as follows.

- ✓ To model longitudinal train dynamics using multibody dynamics formulation, including train-braking dynamics of AA-LRT.
- ✓ To model main parts of electrical braking system for trams used in AA-LRT.
- ✓ To model and test response of the existing PI controller based braking system
- ✓ To develop Model Reference Adaptive controller based braking system and test its performance for disturbance handling
- ✓ To simulate PI and MRAC controllers based braking system of AA-LRT in MathLab Simulink.

1.4 Scope of the Thesis Work

In development of adaptive control based braking system for railway vehicles, mainly the focus area of the thesis is the passenger vehicles used in AA-LRT. Since it is very complicate to model and simulate braking system, working in specific locomotive type is more accurate. This thesis will study and model regenerative and resistance braking control system (Proportional and Integral) of those passenger trams by considering longitudinal forces as a main variable. MathLab Simulink will be the main tool for simulation and testing.

1.5 Methodology

In conducting this thesis the following methods are used to achieve the general and specific objective of the thesis.

- Possible data source assessment to get detail knowledge about the topic, which includes reviewing previous researches, reports, journals, books and other related materials.
- Input information or data collection from different sources in different ways and in different time like visiting ERC office getting Specifications and recorded data; site survey at stations; interviewing train captains and engineers about their experience on braking.
- Analyzing collected data in the way that can be used as a base for the mathematical modeling of railway vehicle braking system.
- Mathematical modeling of the existing braking system i.e. plant modeling and controller modeling.
- After having the exact plant and controller model, developing Model Reference Adaptive Controller Algorithm and implementing it into braking control system model.
- Testing and simulating the mathematical model of the existing braking system with and without the MRAC algorithm on MathLab Simulink.
- Analyzing the performance of the proposed MRAC controller.

The following flow chart summarizes overall methodology

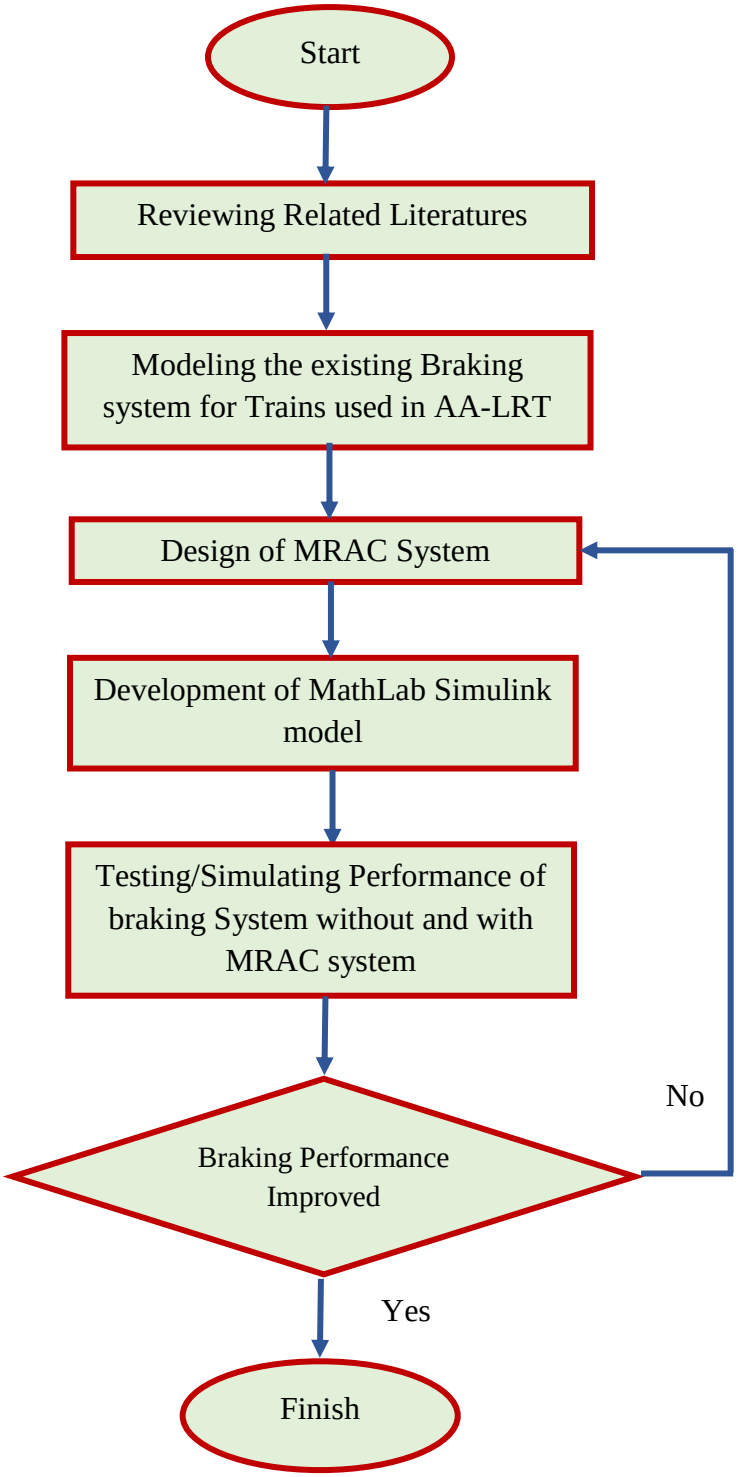

Figure 1.1 Flow Chart for Adopted Research Methodology

1.6 Thesis Contribution

This thesis mainly focus on the application of adaptive controller for railway vehicles braking system for improving braking capacity. The thesis will mainly contribute the following

1. To give a detail analysis about the longitudinal train dynamics impact on train braking, specifically on electrical braking.
2. To study the braking control system used in AA-LRT
3. To show the application of model reference adaptive control system for braking to provide learning capability on nonlinear system.

1.7 Thesis Organization

This thesis is organized in 5 chapters. Chapter one is introductory part which provides clear information about background of the thesis work, statement of the problem, research method and scope of the thesis.

Chapter two is about theoretical background and literature review. This section provides clear understanding of train dynamics, regenerative braking for AC traction motor and model reference adaptive control system. Previous research works which are related to the thesis topic also reviewed in this chapter.

Chapter three is the mathematical modeling and design part of the thesis, in this chapter longitudinal train forces, parts electrical braking system and braking controller will be modeled and the designing and development of the proposed adaptive controller will be discussed.

Chapter four is about MATLAB simulation. After the development of MATLAB Simulink Model depending on the mathematical models developed in chapter three. The simulation result for the models will be discussed and described in terms of performance improvement.

The final chapter is recommendation and conclusion. Here, the thesis work concluded based on the result obtained and discussed in chapter four. Further recommendation for the development of new model or improvement of the result in this thesis is suggested.

Chapter Two

Theoretical Background and Literature Review

In the previous chapter introduction, motivation, objectives, scope and methodology of the thesis were discussed. In the Investigation of literatures to formulate theoretical background, the author explores different books, research papers, journals and websites. The theoretical background and reviewing related literatures are summarized in this chapter in structural manner as follows.

2.1 Theoretical Background

In the previous time there are number of researches conducted on mathematical modeling of railway vehicles braking system, even if their focus area is different. The study of railway vehicle braking is important to investigate in-train forces, safe operation, braking distance and time, and vehicle speed. Railway dynamics is very complicated modeling task since the dynamics is constrained to a lot of internal and external factors. In this research paper next to mathematical model of braking system employed in trains, adaptive control mechanism will be the next focus area. Generally, in this section the following theoretical points will be discussed

- Modeling the wheel rail interaction and longitudinal dynamics
- Electrical Braking : i.e. Specifically Regenerative braking
- Model Reference Adaptive control- MRAC can adapt to changes in locomotive operating conditions, available dynamic braking effort, coupler design, and available wheel/rail adhesion conditions in real time to provide better braking performance than non-adaptive controllers.

2.1.1 Train Dynamics

In studying control of train braking system, it is mandatory to understand the main tractive force characteristics, vertical and lateral train dynamics and other factors which will affect the system.There are three categories of the train dynamics models.

i. **Longitudinal train dynamics models: -** these models are used to predict coupler forces and train speed, distance and time relationships, and useful in the study of train make-up, handling, and the design of braking system and cushioning devices.

ii. **Lateral train dynamics models: -** They are used to study the effects of coupler length and alignment, and vehicle geometry on lateral stability.

iii. **Vertical train dynamics models:** -these models serve as tools to study the heave action of trains under various operating condition [6].

2.1.1.1 Longitudinal Train Dynamics

Longitudinal forces develop from operation of vehicles coupled by spring assemblage (draft gear, cushioning device etc.).The factors that affect longitudinal train forces are, in a gross sense, these:

1) The number of locomotives and cars and their related weights, dimensions, and positions;
2) The grades, or the curvatures over which the train operates;
3) The characteristics of the braking system employed;
4) The speed of the train and the types of throttle used by the engineer in brake manipulation to control the train.

When the train goes from a downgrade to an upgrade, the heavy block will run out rapidly on the train, causing high longitudinal forces and perhaps a braking in two of the train. Reversing the position of the block would reduce the forces. Therefore, when we speak of train handling, train makeup, track geometry investigations, and design of draft gear and cushioning devices, we are often discussing the area of longitudinal train dynamics.

Train Resistance forces

Train resistance, the force required to move a train, is the sum of the rolling resistance on tangent level track, grade resistance and curve resistance of the locomotives and cars [7, 8].

$$F_{train\ resistance} = F_r + F_{cr} + F_g \tag{2.1}$$

Where

$F_{train\ resistance}$= Train resistance forces

F_r = Train rolling resistance force

F_{cr}= Curve resistance force

F_g=Gradient resistance force

a. Rolling Resistance

Rolling Resistance is the sum of the forces that must be overcome by the tractive effort of the locomotive to move a railway vehicle on level tangent track in still air at a constant speed.

In general, rolling resistance of a train, F_r (in Newton.), can be calculated using an empirical expression as follows:

$$F_r = A + BV + CV^2 \tag{2.2}$$

Where A, B & C are coefficients defining the different resistive forces that are either independent, dependent or affected by the square of the train speed V.

Where

F_r= Train rolling resistance force

A = Journal resistance coefficient which depends on railcar weight and number of axles

B= Flanging resistance coefficient which depends on flanging friction and the train speed

C= Drag coefficient based on the shape of the front of the train and

V= Train speed

The formula for rolling resistance can be approximately simplified according to France adopted formula [8].

$$r = \left(1.5\sqrt{\frac{10}{e}} + \frac{V^2}{120e}\right) \frac{Kilogram}{tonne} \tag{2.3}$$

Where e=axle load in tonne, so rolling resistance force become

$$F_r = 9.81\, r\, W \quad Newtons \tag{2.4}$$

Where W is weight of the train in tonnes

b. Grade Resistance

Going uphill produces a resistive force while a downgrade produces an accelerating (negative resistive) force. After a portion of the tractive force is used to overcome the grade resistance, the excess is used to accelerate the train. If the grade resistance increases after the balance speed is reached, the train will slow down. If the grade keeps on increasing, the train will slow to a speed that the engine cannot sustain and it will stall and stop [7].

$$F_g = 1000 W sin\theta \qquad Newtons$$

$$F_g = \pm WD \qquad Newtons \tag{2.5}$$

Where W = Weight of the train in Newton, $D = 1000 sin\theta$= Slope

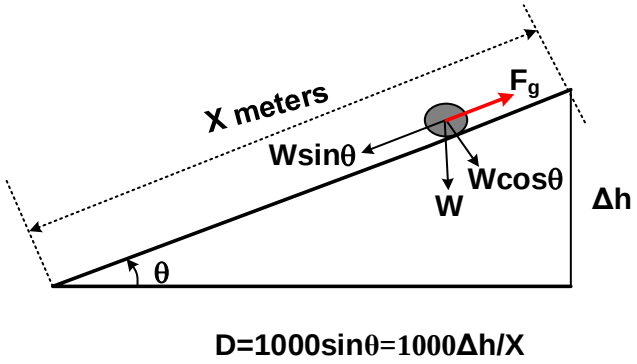

Figure 2.1 Grade Resistance of Moving Body [7]

c. Curve resistance:

Vehicle running at a speed V with a radius of R experience centrifugal acceleration of and this acceleration is the reason for undesired effect like passenger discomfort, displacement of wagon load, risk of overturning and high lateral force on the track which increases curve resistance, risk of rail tilting and risk of lateral displacement of whole track [7,8].

Figure 2.2 Curve in Railway Track [7]

For Radius less than 150 meters

$$F_c = 9.81\left(\frac{700}{R}\right)W \quad Newtons \tag{2.6}$$

For Radius greater than 150 meters

$$F_c = \frac{6.5\,W}{R-55} \quad Newtons \tag{2.7}$$

2.1.2 Railway Vehicles Braking System

For railway vehicles various brake systems have been developed, whose construction, design and operation depend on many factors such as running speed, axle load, type, construction and technical characteristics of vehicles, traffic conditions, etc. Depending on how the command actions are performed and according to the mean that braking forces are basically developed, braking system is divided in to [9].

A. Handbrakes

Which are applied by hand action to a wheel or lever on the vehicle. Nowadays are generally used for securing unattended or unpowered vehicles against unplanned movement, not for braking actions while operating. That is why usually it is known as parking brakes [9]. Parking brake is provided to prevent train at standstill from coasting [5].

B. Hydraulic brakes

Which act using hydraulic oil and, depending on the achievement of braking forces, there may be hydrostatic, when is due to oil pressure increasing or hydrodynamic when the kinetic energy of the vehicle is converted in the rotor of a hydraulic pump in heat which is dissipated through the oil cooling system [10].

C. Rail (track) brakes

Which are usually electric commanded and the braking force is achieved due to strong magnetic forces induced by large electromagnets hung under the vehicle's bogie, over the top surface of the rails. If the braking forces are generated by the frictional forces between the electromagnets and rails it is an electromagnetic rail brake. If the electromagnetic fields generate eddy currents in the rails, creating forces acting in the opposite direction of the movement of the train, it is a

linear eddy current brake system. On the same principle is the rotary eddy currents brake system, the metallic mass being either the wheels, or discs attached to the wheel sets [9].

D. Electric braking

Which is based on the reversibility of the electric engine, in particular the electric traction motors are reconnected in such a way that they act as generators which provide braking effort. Practically, the kinetic and/or the potential energy (while running on slopes) are converted into electric energy. If the power generated during braking is dissipated as heat through on-board resistors it is about rheostat braking. On electric railways, it is also possible to convert the energy of the train back into usable power by diverting the braking current into traction supply line, this being the case of regenerative braking [13].

Electrical Braking for Alternative Current (AC) Traction Motors

The energy put into accelerating a train and into moving it uphill is "stored" in the train as kinetic and potential energy. In vehicles with electric traction motors (this includes electric, diesel-electric and hybrid stock) a great part of this energy can be reconverted into electric energy by using the motors as generators when braking. The electric energy is transmitted "backwards" along the conversion chain and fed back into the catenary. This is known as regenerative braking and widely used in railways [11].

The energy recovered by dynamic braking is used for different purposes: on-board purposes (auxiliaries or comfort functions). On-board demand is usually far too low to consume all the energy supplied. Energy is fed back into catenary to be used by other trains motoring close enough (in a section of track supplied by the same substation). If DC substations are equipped with thyristor inverter units, they can feed back energy into the national grid [11].

In AA-LRT Regenerative brake should be preferably applied as service brake for vehicles. Role of regenerative brake should be utilized to a maximum extent and return energy back to power network. In case of insufficiency in regenerative braking force or failure of regenerative brake, resistance brake will be automatically put into service for compensation [5].

Braking resistance is used under the resistance working condition of traction inverter, to consume the energy generated by traction motor under braking condition when regenerative braking is not possible, the design of braking resistance matches with the electric parameter of

traction inverter, one traction inverter is equipped with one braking resistance cabinet, including two sets of braking resistance modules inside [21].

2.1.3 Main Parts of Electrical Traction and Braking System.

2.1.3.1 Induction traction motors

The robustness of induction motors of squirrel cage type and its reduced maintenance and operation cost has already attracted the traction railway applications. The development of power electronics such as GTO or IGBT has led to application of induction motors for traction purposes through invention and accurate control of PWM controlled variable voltage variable frequency (VVVF) inverters which give a VVVF output from a DC input. Therefore, the need for an in-built series characteristic for self-regulation becomes redundant if an induction motor is fed with VVVF supply because it eliminates the main draw backs of an induction motor such as switching's in speed and torque control methods [13,14].

By regenerative braking, the induction machine operates as generator, the DC/AC converter – the motor side converter - becomes "rectifier" using the voltage of the DC – link. The AC/DC converter - the line-side converters – becomes inverter and transfers the electrical power to the grid [15]. The figure below shows the motor and generator action of induction motors.

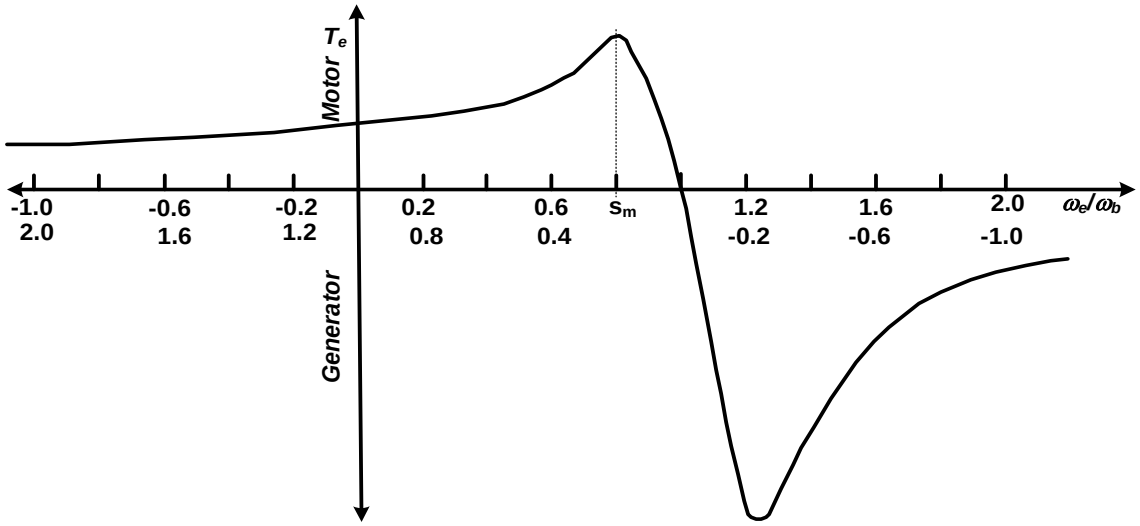

Figure 2.3 Typical Torque-Speed Curve for Induction Machine [15]

$$S = \frac{\omega_S - \omega_m}{\omega_s} \tag{2.8}$$

Where

S= Slip, ω_S=synchronous speed (radians per second),ω_m= rotor mechanical speed (radians per second)

The three-phase asynchronous motor is an induction motor based on the generation of rotating magnetic fields by means of the stator windings, which induce electric currents in the rotor windings. Due to the interaction between these induced currents and the magnetic fields, forces are generated in the conductors that produce a motor torque. If the rotor rotates at the same speed as the magnetic fields, there is no variation of flux passing through the turns of the rotor and the induced current is zero. For a motor torque to be produced there needs to be a difference (slip) between the angular velocities of the magnetic field and the rotor [16]. If the slip is the in the negative region the motor is acting as generator.

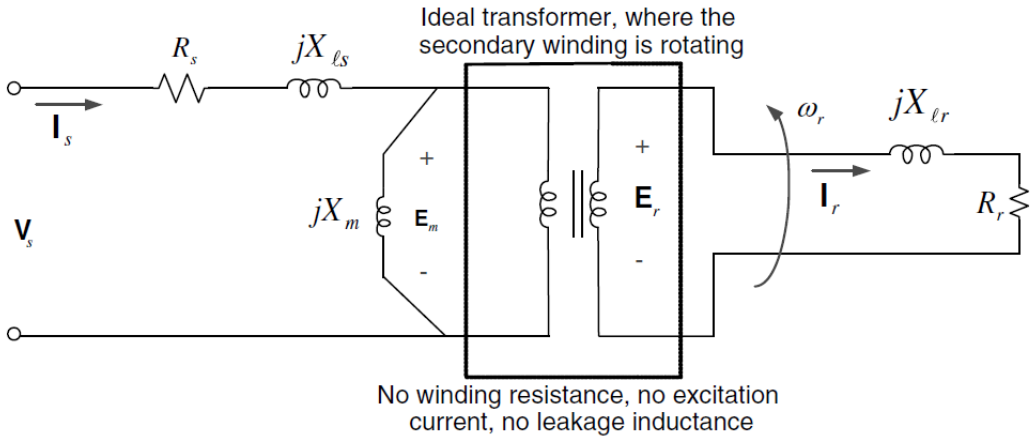

Figure 2.4 Steady State per Phase Equivalent Circuit of Squirrel Cage Motor [24]

Induction motor can be modeled drawn as Figure 2.4 using the equivalent circuit of an ideal transformer. In the figure, R_s stands for the stator winding resistance, X_{ls} stands for the stator winding leakage reactance, X_m stands for the excitation reactance, X_{lr} stands for the rotor winding leakage reactance, and R_r stands for the rotor winding resistance. The above picture Figure 2.4 can be simplified to equivalent circuit with shorted rotor as shown in Figure 2.5.

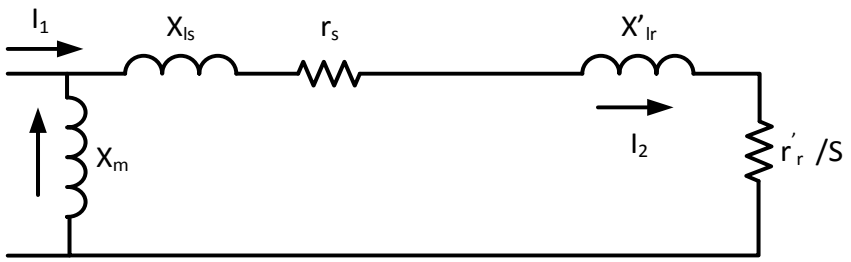

Figure 2.5 Induction Motor Simplified Equivalent Circuit with Shorted Rotor [24]

The total power crossing the air-gap is divided in to two; the first being converted to mechanical power while the rest is loss in rotor copper winding.

$$P_{ag} = 3\frac{P}{2}I_2^2\frac{r_r}{s} \tag{2.9}$$

$$P_{Cu\ loss} = 3\frac{P}{2}I_2^2 r_r \tag{2.10}$$

$$P_{mech} = P_{ag} - P_{cu\ loss} \tag{2.11}$$

$$P_{mech} = 3\frac{P}{2}\frac{r_r}{s}I_2^2(1-s)$$

$$T_m = \frac{P_{mech}}{\omega_r} = 3\frac{P}{2}\frac{1}{\omega_r}\frac{r_r}{s}I_2^2(1-s) \tag{2.12}$$

$$\omega_r = (1-s)\omega$$

$$T_m = 3\frac{P}{2}\frac{1}{\omega}\frac{r_r}{s}I_2^2$$

$$I_2 = \frac{V_1}{\sqrt{\left(\frac{r_r}{s}+r_s\right)^2 + (\omega L_s + wL_r)^2}} \tag{2.13}$$

$$T_m = 3\frac{P}{2}\frac{r_r}{\omega s}\frac{(V_1)^2}{\left(\frac{r_r}{s}+r_s\right)^2 + (\omega L_s + \omega L_r)^2} \tag{2.14}$$

Where

$I_1 = Stator\ circuit\ current$

$P_{ag} = Total\ air-gap\ power$

$I_2 = Rotor\ current\ reffered\ to\ stator$

$P_{Cu\ loss} = Copper\ loss\ power$

$r_s = Stator\ circuit\ winding\ resistance$

$P_{mech} = Mechanical\ power$

$r_r = Rotor\ winding\ resistance\ refered\ to\ stator$

$S = slip$

$L_s = Stator\ winding\ inductance$

$L_r =$ $\omega = Frequency\ of\ the\ input\ voltage$

$Rotor\ winding\ inductance\ refered\ to\ stator$

By considering equation 2.14 the speed of the induction motor can be adjusted by varying the values of the following motor parameters and variables

- Varying the input stator voltage of the induction motor
- Varying the input frequency of the induction motor
- Adding external resistor to the rotor circuit (for wound type induction motor)
- Simultaneous variation of the stator voltage and frequency
- Changing number of poles

2.1.3.2 Traction Power Converter

AC drives receive AC power and convert it to an adjustable frequency, adjustable voltage output for controlling motor operation. The three common inverter types are current source inverter (CSI), voltage source inverter (VSI) and pulse width modulation inverter (PWM) [25].

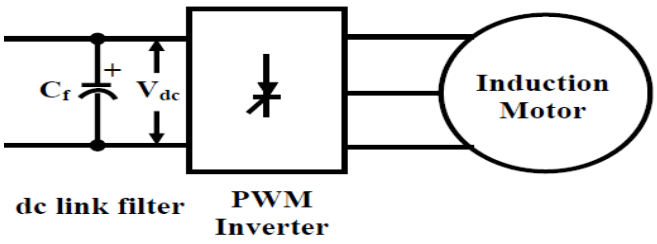

Figure 2.6 PWM Inverter Fed Induction Motor Drive [26]

The converter is mainly to provide variable frequency power supply and variable voltage power supply to the traction motor of the light rail vehicles for it to perform its functions such as traction, braking and anti-skidding and anti-slipping functions. The variable voltage variable frequency supply for an induction motor drive consists of an inverter (dc to variable voltage/variable frequency ac), the voltage and frequency can both be controlled in a pulse-width-modulated (PWM) inverter as shown in Figure 2.6. The dc link filter consists of a capacitor to keep the input voltage to the inverter stable and ripple-free. The output voltage and frequency can be controlled using sinusoidal pulse width modulation method [26, 27]

Sinusoidal PWM

Figure 2.7 (a) explains the general principle of SPWM, where an isosceles triangle carrier wave of frequency f_c is compared with the sinusoidal modulating wave of fundamental frequency f, and the points of intersection determine the switching points of power devices. For example, for phase-a, voltage (V_{a0})is obtained by switching ON Q1 and Q4 of half-bridge inverter, as shown in the Figure 2.7 . Assuming that f << fc, the pulse widths of V_{a0} wave vary in a sinusoidal manner. Thus, the fundamental frequency is controlled by varying f and its amplitude is proportional to the command modulating voltage. The Fourier analysis of the V_{a0} wave can be shown to be of the form:

$$V_{a0} = 0.5mV_d \sin(2\pi ft + \phi) + harmonics \qquad (2.15)$$

Where m = modulation index and ϕ = phase shift of output, depending on the position of the modulating wave.

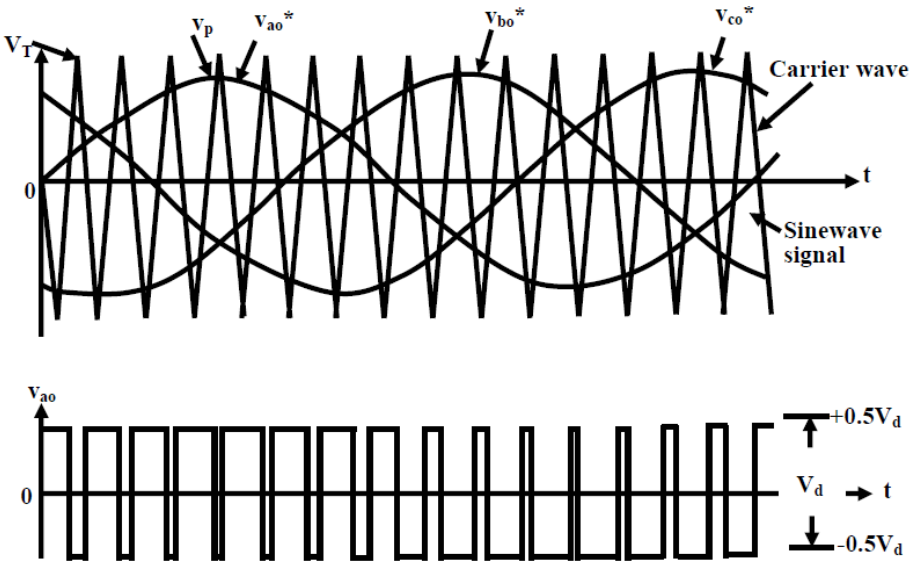

Figure 2.7 (a) Principle of Sinusoidal PWM for Three-Phase Bridge Inverter [27].

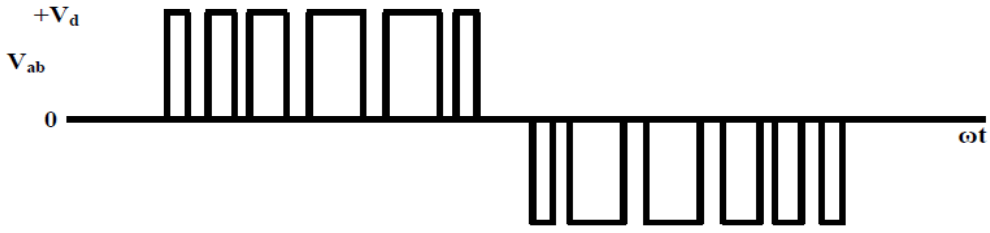

Figure 2.7 (b) Line Voltage Waves of PWM Inverter [26]

The modulation index m is defined as

$$m = \frac{V_P}{V_T} \tag{2.16}$$

Where

V_P= peak value of the modulating wave and V_T = peak value of the carrier wave. Ideally, m can be varied between 0 and 1 to give a linear relation between the modulating and output wave. The inverter basically acts as a linear amplifier. The line voltage waveform is shown in Figure 2.7(b) [26].

2.1.3.3 Variable Voltage Variable Frequency Control of Induction Motor.

As it is discussed in section 2.1.3.3 the speed of induction motor can be controlled using different mechanisms, V/Hz (volt per hertz) control system is one of them and widely used for different application including railway vehicles [34]. Synchronous speed can be controlled by varying the supply frequency. Voltage induced in the stator is $E1 \propto \Phi f$where Φ is the air-gap flux and f is the supply frequency. As we can neglect the stator voltage drop we obtain terminal voltage $V1 \propto \Phi f$. Thus reducing the frequency without changing the supply voltage will lead to an increase in the air-gap flux which is undesirable. Hence whenever frequency is varied in order to control speed, the terminal voltage is also varied so as to maintain the V/f ratio constant. Thus by maintaining a constant V/f ratio, the maximum torque of the motor becomes constant for changing speed [26] [27]. To vary the speed by making the maximum torque constant, the maximum torque equation will be

$$T_{\max(s=1)} = 3\frac{P}{2}\frac{r_r}{\omega s}\frac{(V_1)^2}{\left(\frac{r_r}{s}+r_s\right)^2+(\omega L_s + wL_r)^2} \tag{2.17}$$

$$T_{\max(S=1)} = \frac{3}{2}P\frac{V_1^2}{\omega(\omega L_s + \omega L_r)}$$

$$T_{max} = \frac{3}{2}P\frac{1}{(L_s+L_r)}\frac{V_1^2}{\omega^2} = K\frac{V_1^2}{\omega^2} \tag{2.18}$$

$I_2 = Rotor\ current\ reffered\ to\ stator$

$r_s = Stator\ circuit\ winding\ resistance$

Where

$r_r = Rotor\ winding\ resistance\ refered\ to\ stator$

$T_{max} = Maximum\ torque$

$L_s = Stator\ winding\ inductance$

$S = slip$

$L_r = Rotor\ winding\ inductance\ refered\ to\ stator$

$P = number\ of\ poles$

$\omega = Frequency\ of\ the\ input\ voltage$

$I_1 = Stator\ circuit\ current$

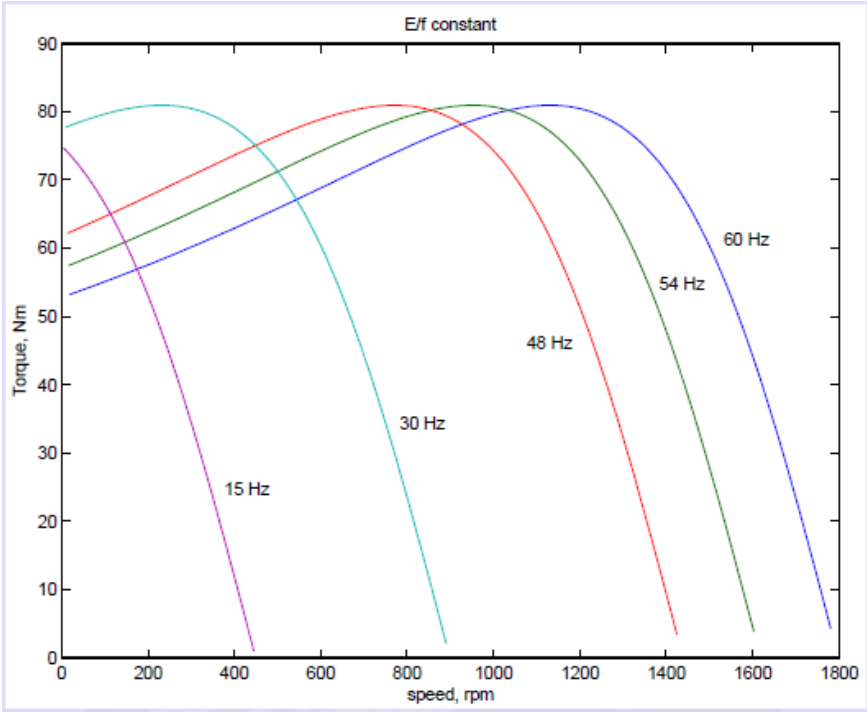

Figure 2.8 Torque-Speed Curves with E/f Held Constant [29]

If voltage to frequency ratio is kept constant, the maximum torque remains constant.

Open loop and closed loop Volts/Hertz control

Open loop Volts/Hz control of an induction motor is far the most popular method of speed control because of its simplicity and these types of motors are widely used in industry. For adjustable speed applications, frequency control is natural. However, voltage is required to be

proportional to frequency so that the stator flux remains constant if the stator resistance is neglected [29] however some problems encountered in the operation of this open loop drive like:

- Speed of the motor cannot be controlled precisely, because the rotor speed will be slightly less than the synchronous speed and that in this scheme the stator frequency and hence the synchronous speed is the only control variable.
- Slip speed, being the difference between the synchronous speed and the electrical rotor speed, cannot be maintained, as the rotor speed is not measured in this scheme. This can lead to operation in the unstable region of the torque-speed characteristics.

These problems are to an extent overcome by having an close loop in the induction motor drive, in which the actual rotor speed is compared with its commanded value, and the error is processed through a controller usually a PI controller and a limiter is used to obtain the slip-speed command[29, 30].

Closed loop control - When accuracy in speed response is a concern, closed loop speed control can be implemented with the constant v/f principle through the regulation of slip speed. A PI controller is employed to regulate the slip speed of the motor to keep the motor speed at its set value. By adding a sensor signal for the measured speed, and a reference for the stator speed adjustment in the steady state. VVVF inverters can have more accuracy in speed, but this type of control cannot be used for high performance applications [28, 30].

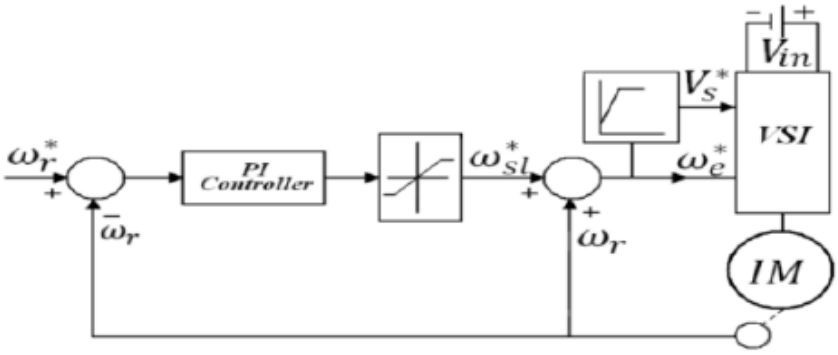

Figure 2.9 Closed Loop Speed Control of Induction Motor [31]

The block diagram of system configuration is shown in Figure 2.9. An error signal obtained by the difference between the actual speed and reference speed. The error was then processed in a

controller (Proportional and Integral). The output then sets the inverter frequency as well as the modulation index. The slip speed command, is regulated by a slip regulator. The PWM based three phase inverter frequency was determined from the synchronous speed. The synchronous speed was calculated by summing actual speed to the slip speed, frequency generates the reference signal for the V/F control of the induction motor terminal voltage Vs. The drive finally gets settles at slip speed (motor torque balances the load torque) [31].

For trams used in AA-LRT traction inverter adopts the control strategy of the advanced VVVF control, and the changes of electrical parameters of the motor impose very little influence on the control characteristics. The VVVF control has advantages of good output characteristics and rapid dynamic response, and it has relatively simple control system, which is an AC speed regulation method with excellent static and dynamic performance [22].

2.1.3.4 Proportional Integral (PI) Controller

At present, the PI controller is most widely adopted in industrial application due to its simple structure, easy to design and low cost.

$$U(s) = K_p e(s) + \frac{K_i e(s)}{s} \tag{2.19}$$

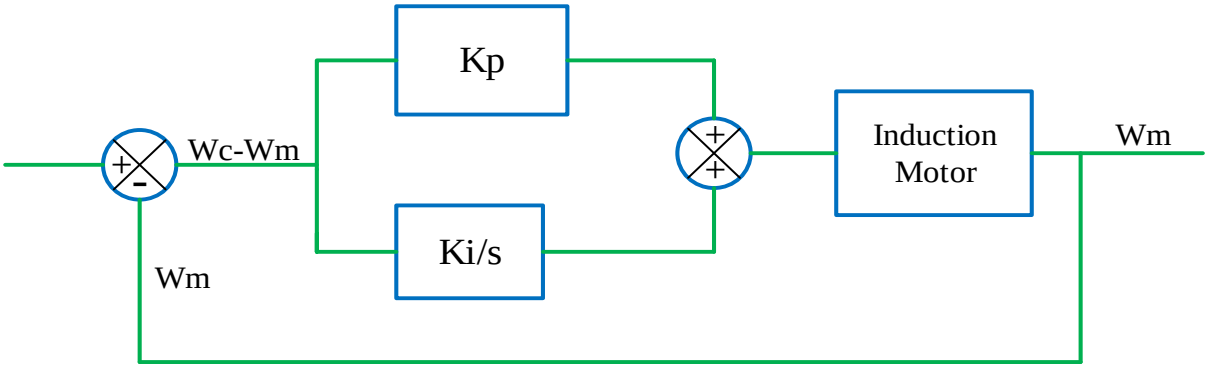

Figure 2.10 Proportional Integral (PI) Controller

Figure 2.10 Proportional Integral (PI) Controller is an integral error compensation scheme, the output response depends in some manner upon the integral of the actuating signal. This type of compensation is introduced by using a controller which produces an output signal consisting of two terms, one proportional to the actuating signal and the other proportional to its integral. Such a controller is called proportional plus integral controller or PI controller [32].

PI controllers are very often used in industry, especially when

1. Speed of the response is not an issue.
2. There is only one energy storage in process (capacitive or inductive)
3. There are large transport delays in the system

Despite the above advantages, the PI controller fails when the controlled object is highly nonlinear and uncertain. PI controller will eliminate forced oscillations and steady state error resulting in operation of on-off controller and P controller respectively. However, introducing integral mode has a negative effect on speed of the response and overall stability of the system, as the high starting overshoot, sensitivity to controller gains and sluggish response due to sudden disturbance. Thus, PI controller will not increase the speed of response. It can be expected since PI controller does not have means to predict what will happen with the error in near future [32, 33].

But train braking/speed control system is mainly dependent on controller response time, large disturbances and noise are present during operation of the process. So there should be another fast response controller which can avoid the above problems.

2.1.4 Model Reference Adaptive Control

Adaptive Control covers a set of techniques which provide a systematic approach for automatic adjustment of controllers in real time, in order to achieve or to maintain a desired level of control system performance when the parameters of the plant dynamic model are unknown and/or change in time [18].

2.1.4.1 Direct and Indirect Adaptive Controllers

The first categorization of adaptive control system is based on the control law used for adaptation of the system.

- **Indirect adaptive control**: in this approach, the plant parameters are estimated on-line and used to calculate the controller parameters if a model of the plant is estimated on line from

the available input-output measurements [17]. Indirect adaptive control scheme can be viewed as a real-time extension of the controller design [18].

- **Direct adaptive control**: in this approach, the plant model is parameterized in terms of the controller parameters that are estimated directly without intermediate calculations involving plant parameter estimates [19]. When the plant parameters are unknown or change in time, in order to achieve and to maintain the desired performance, an adaptive control approach has to be considered, such a scheme known as Model Reference Adaptive Control (MRAC) This scheme is based on the observation that the difference between the output of the plant and the output of the reference model (called subsequently plant-model error) is a measure of the difference between the real and the desired performance [17, 18].

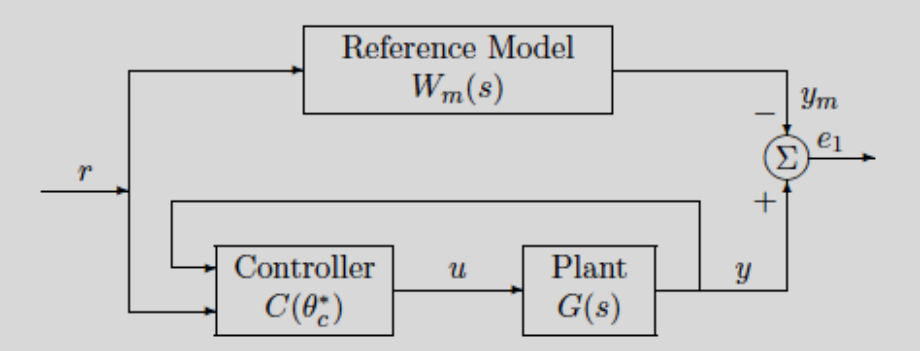

Figure 2.11 Block Diagram of MRAC System [17]

- This information (together with other information) is used by the adaptation mechanism (subsequently called parameter adaptation algorithm) to directly adjust the parameters of the controller in real time in order to force asymptotically the plant model error to zero. Note that in some cases, the reference model may receive measurements from the plant in order to predict future desired values of the plant output. For this research work Model Reference Adaptive Control (direct*)* will be used, since the plant parameters are unknown and time varying.

2.1.4.2 Adaptation Mechanism

Adaptation Mechanism: It is used to adjust the parameters in the control law. Adaptation law searches for the parameters such that the response of the plant which should be same as the reference model. It is designed to guarantee the stability of the control system as well as conversance of tracking error to zero. The most widely used techniques are MIT rule and

Lyapunov theory. Due to it is simplicity and modernization in this paper MIT rule will be used as adaptation mechanism/ rule [19, 20].The MRAC control strategy is obtained using gradient approach of MIT rule.

The MRAC control strategy is obtained using gradient approach of MIT rule. According to gradient approach, a cost function ($\psi(\phi)$) is decided in terms of tracking error (e) as shown below. The tracking error is defined as error between output of reference model and output of plant [33].

$$e = y(t) - y_m(t) \tag{2.20}$$

$$\psi(\phi) = \frac{1}{2}e^2(\phi) \tag{2.21}$$

According to the MIT rule, rate of change of ϕ is directly proportional to negative gradient of cost function, as shown in the following equations:

$$\frac{d\phi}{dt} = -\gamma\frac{\partial\psi}{\partial\phi} \tag{2.22}$$

$$\frac{d\phi}{dx} = -\gamma e\frac{\partial e}{\partial\phi} \tag{2.23}$$

Where,

ϕ = controller parameter vector, e = tracking error, γ= adaptive gain and $\frac{\partial e}{\partial\phi}$ =sensitivity derivative.

Design of MRAC

The output of a PI controller in accordance to the error as input is given as

$$u(s) = \left[K_p + \frac{K_i}{s}\right]e(s) \tag{2.24}$$

Since it is assumed that the structure of the plant is known even though there exact parameters are not known, now in this case the motor transfer function is of first order, where

$$\frac{y(s)}{u_c(s)} = \frac{b}{s+b} \tag{2.25}$$

After introduction of the PI controller to the plant the structure becomes

$$\frac{y(s)}{u_c(s)} = \frac{b(k_p s + K_i)}{s^2 + s(a + bk_p) + bk_i} \tag{2.26}$$

So the reference model can also be assumed of the form as so let it be

$$\frac{y_m(s)}{u_c(s)} = \frac{b_{m1}s + b_{m2}}{s^2 + a_{m1}s + a_{m2}} \tag{2.27}$$

Now the MIT rule can be applied to motor to obtain the controller parameters. Since the controller parameter vector $u = [k_p, k_i]$ the MIT rule can be written as will be dividing up into two parts as follows

$$\frac{dK_p}{dt} = -\gamma_p\left(\frac{\partial\psi}{\partial k_p}\right) = -\gamma_p(\frac{\partial\psi}{\partial e})(\frac{\partial e}{\partial y})(\frac{\partial y}{\partial k_p}) \tag{2.28}$$

$$\frac{dK_i}{dt} = -\gamma_i\left(\frac{\partial\psi}{\partial k_i}\right) = -\gamma_i(\frac{\partial\psi}{\partial e})(\frac{\partial e}{\partial y})(\frac{\partial y}{\partial k_i}) \tag{2.29}$$

But

$$e = y(t) - y_m(t) \;\Rightarrow\; \frac{\partial e}{\partial y} = 1 \tag{2.30}$$

And

$$\frac{\partial\psi}{\partial e} = e \tag{2.31}$$

$$\frac{dK_p}{dt} = -\gamma_p\left(\frac{\partial\psi}{\partial k_p}\right) = -\gamma_p e(\frac{\partial y}{\partial k_p}) \tag{2.32}$$

$$\frac{dK_i}{dt} = -\gamma_i\left(\frac{\partial\psi}{\partial k_i}\right) = -\gamma_i e(\frac{\partial y}{\partial k_i}) \tag{2.33}$$

Where

ϕ = Controller parameter vector

e = Tracking error

K_p= Proportional controller

K_i= Integral controller gain

$\frac{\partial e}{\partial \phi}$ = Sensitivity derivative

y = Plant output

γ_p= Adaptive gain for proportional controller

γ_i= Adaptive gain for integral controller

Now to find $\frac{\partial y}{\partial k_p}$ and $\frac{\partial y}{\partial k_i}$ equation 2.26 can be used differentiating it as follows

$$\frac{y(s)}{u_c(s)} = \frac{b(k_p s + K_i)}{s^2 + s(a + bk_p) + bk_i}$$

$$y(s^2 + s(a + bk_p) + bk_i) = b(k_p\, s + K_i)u_c(s)$$

Differentiating Eq.2.27 w. r. t k_p

$$\left[y\frac{\partial}{\partial k_p}(s^2 + s(a + bk_p) + bk_i)\right] + \left[\frac{\partial y}{\partial k_p}(s^2 + s(a + bk_p) + bk_i)\right] = \left[\frac{\partial}{\partial k_p} b(k_p\, s + K_i)u_c(s)\right]$$

$$\Rightarrow \qquad \frac{\partial y}{\partial k_p} = b\frac{s}{(s^2 + s(a + bk_p) + bk_i)}(u_c - y) \tag{2.34}$$

Similarly Differentiating Eq.2.27 w. r. t k_i

$$\left[y\frac{\partial}{\partial k_i}(s^2 + s(a + bk_p) + bk_i)\right] + \left[\frac{\partial y}{\partial k_i}(s^2 + s(a + bk_p) + bk_i)\right] = \left[\frac{\partial}{\partial k_i} b(k_p\, s + K_i)u_c(s)\right]$$

$$\Rightarrow \qquad \frac{\partial y}{\partial k_i} = b\frac{1}{(s^2 + s(a + bk_p) + bk_i)}(u_c - y) \tag{2.35}$$

Substituting

$$\frac{dK_p}{dt} = -\gamma_p\left(\frac{\partial \psi}{\partial k_p}\right) = -\gamma_p e\frac{bs}{(s^2 + s(a + bk_p) + bk_i)}(u_c - y) \tag{2.36}$$

$$\frac{dK_i}{dt} = -\gamma_i\left(\frac{\partial \psi}{\partial k_i}\right) = -\gamma_i e\frac{b}{(s^2 + s(a + bk_p) + bk_i)}(u_c - y) \tag{2.37}$$

From these two equation the gain parameters cannot be found out since the value of a & b are not known. So defining

$$a_{m1} = a + bk_p \tag{2.38}$$

$$a_{m2} = bk_i \tag{2.39}$$

$$\gamma^l = \frac{\gamma b}{a_{m1}} \tag{2.40}$$

$$\frac{dK_p}{dt} = -\gamma_p^l e \frac{a_{m1} s}{\left(s^2 + s\left(a + bk_p\right) + bk_i\right)} (u_c - y) \tag{2.41}$$

$$\frac{dK_i}{dt} = -\gamma_i^l e \frac{a_{m1}}{\left(s^2 + s\left(a + bk_p\right) + bk_i\right)} (u_c - y) \tag{2.42}$$

By using these equations the MRAC will developed in the next chapter as a solution to improve problems related to other robust controllers.

2.2 Literature Review

Different researches conducted in the railway industry to guarantee safe operation and to have efficient handling of trains. In this paper some previous works conducted by some researchers will be reviewed accordingly, since there are no much researches on application of adaptive control for railway vehicles braking system.

In [9], the authors have presented the current status of their research concerning the simulation of long train longitudinal dynamics, pointing the attention to the braking phase. The paper present simplified models used to evaluate, in a convenient time-saving way how train composition, buffers mechanical features, braking plant design and other key parameters may influence the longitudinal behavior of the convoy. Longitudinal forces exchanged by buffers along the train are usually calculated through a lumped model where each wagon is modelled as a single lumped inertia, neglecting additional degrees of freedom due to bogies, suspension system, wheel-rail interaction, etc. This simplified approach is thus used to predict wagons and train compositions with the worst loading condition during the braking phase. This paper helps to understand the impact of suspension between two rail cars.

This research [4] focuses on the application of MRAC for better controlling wheel-rail interface dynamics and longitudinal train forces in order to bring a moving train to stop without exceeding the maximum wheel longitudinal creep forces or the allowable inter-train dynamics. The author tried to develop a relationship between creep forces, creepage, and the braking torque for different weights of the locomotive using the longitudinal train dynamic model; and to extensively study the interaction between dynamic braking control and dynamic braking provided by the traction motors. The author also develop MRAC control mechanism for both direct current and alternating current traction motors used in freight locomotives. Finally he tried to simulate the braking performance using MathLab .The main drawback of this paper is, the design and simulation of the controller is not based on actual field data.

Regenerative braking system is a system which converts mechanical energy to electrical energy during braking action. It is an important system for the vehicle such as hybrid and electric train. This paper [21], mainly concerned about the potential of regenerative braking system on the reduction of energy consumption. The author calculate the generated energy by using

regenerative braking from Ayat to Tor-hailoch of the east-west line of Addis Ababa LRT of the stations. This paper give good impression about regenerative braking in AA-LRT.

In [22], the author have presented an anti-slip re-adhesion control method using vector control without speed sensor. Their method focuses on the current from each induction motor for multiple motor drive systems with one inverter, and it detects the torque current differences between two induction motors by setting a threshold. If the assumed threshold is reached, the controller reduces current to both traction motors uniformly since there is one inverter. A fixed threshold of 30 Amps is assumed for all simulations. This is not realistic however because the threshold should be a function of speed. Also, the study includes only a sudden drop of 10% of adhesion force that is not sufficient to prove the efficiency of the control method.

Sometimes conventional feedback controllers may not perform well online because of the variation in process dynamics due to nonlinear actuators, changes in environmental conditions and variation in the character of the disturbances. To overcome the above problem, in [20] the authors come up with designing of a controller for a second order system with Model Reference Adaptive Control (MRAC) scheme using the MIT rule for adaptive mechanism. In this rule, a cost function is defined as a function of error between the outputs of the plant and the reference model, and controller parameters are adjusted in such a way so that this cost function is minimized. The designed controller gives satisfactory results, but is very sensitive to the changes in the amplitude of reference signal. The performances of the proposed control algorithms are evaluated and shown by means of simulation on MATLAB and Simulink.

Chapter Three

Mathematical Modeling and Development of Adaptive Controller

In this chapter longitudinal train dynamics, main parts of electrical braking system, proportional and integral controller will be modeled mathematically. After having model of the existing system adaptive controller will be developed accordingly.

3.1 Longitudinal Train Dynamics Modelling for AA-LRT

Addis Ababa Light Rail Transit (AA-LRT) is consisting of two railway lines E-W and N-S, with total length of 31.025km.These two lines operate on the same rail track in downtown area (Stadium to Lideta) for a total length of 2.662km. The entire line has 39 stations, including 9 elevated stations (5 in the section that uses the same rail, 1 on E-W line, and 3 on S-N line), 2 underground stations, 1 semi-underground, and the rest are all ground stations [23]. In this section, forces which will affect longitudinal motion of the train will be discussed.

3.1.1 Train Resistance Forces

Braking distance and time are dependent on deceleration of the train under applied braking force, the required braking force to stop the train should overcome different forces. Therefore, in order to have efficient and effective braking system, it is important to model train longitudinal dynamics

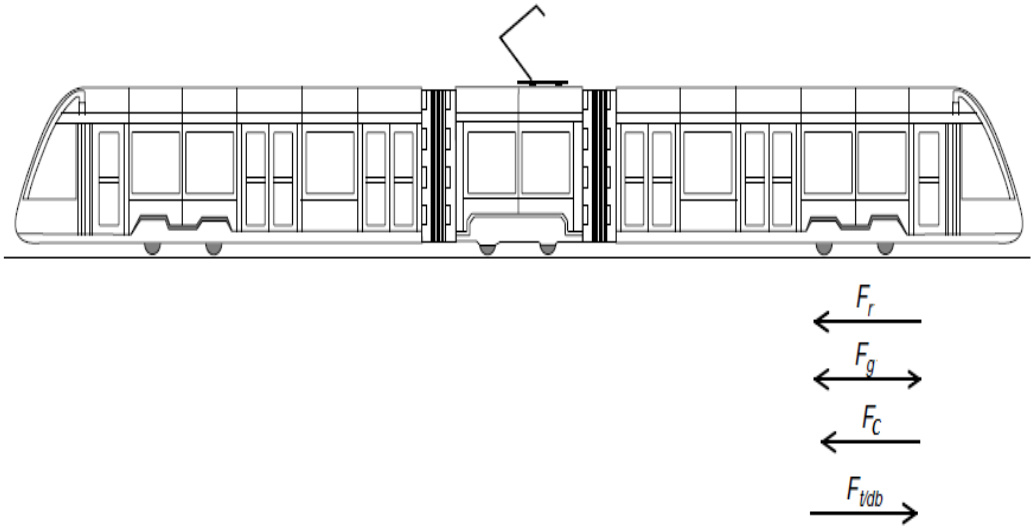

.

Figure 3.1 Longitudinal Forces Acting on Railway Vehicle

While supply power is turned off during electrical braking, force of braking can be expressed as the sum of resistance forces as shown in equation (3.1).

$$F_{rb} = -(F_r + F_a + F_{cr} + F_g)$$

Where

F_{rb}= Train resistance forces

F_r = Train rolling resistance force

F_a = Acceleration force

F_{cr}= Curve resistance force

F_g=Gradient resistance force

a. Rolling Resistance

The rolling resistance is a function of the total mass of the train and the rolling resistance coefficient.

$$F_r = 9.81\, r\, W \quad Newtons$$

$$r = \left(1.5\sqrt{\frac{10}{e}} + \frac{V^2}{120e}\right) \quad Kilogram/tonne$$

For trams used in AA-LRT e= 11 tonne, overload weight W=63.03 tonne and train speed V=70km/hr.

$$r = \left(1.5\sqrt{\frac{10}{11}} + \frac{70^2}{120 * 11}\right) \quad Kilogram/tonne$$

$$r = 5.14 \quad Kilogram/tonne$$

Calculating force of rolling resistance

$$F_r = 9.81\, r\, W$$

$$F_r = 9.81 * 5.14 * 63.03 \quad Newton$$

$$F_r = 3179.6 \qquad Newtons$$

b. Grade Resistance

The gradient resistance depend on the weight of the train and the size of the gradient to which the train is climbing. Gradient distribution of AA-LRT over the main lines is stated as follows in the Figure 3.2.

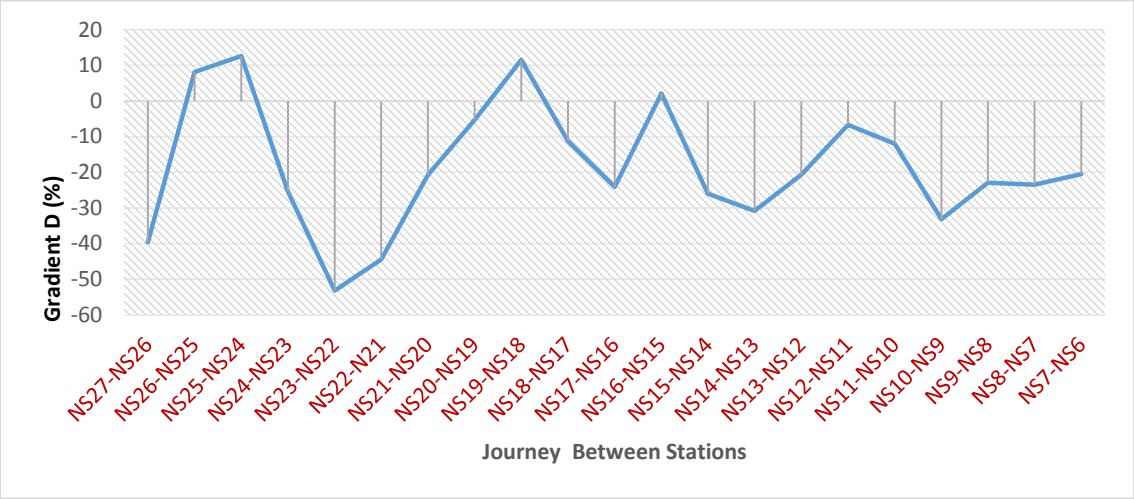

Figure 3.2 Gradient Distribution on North-South LRT Line

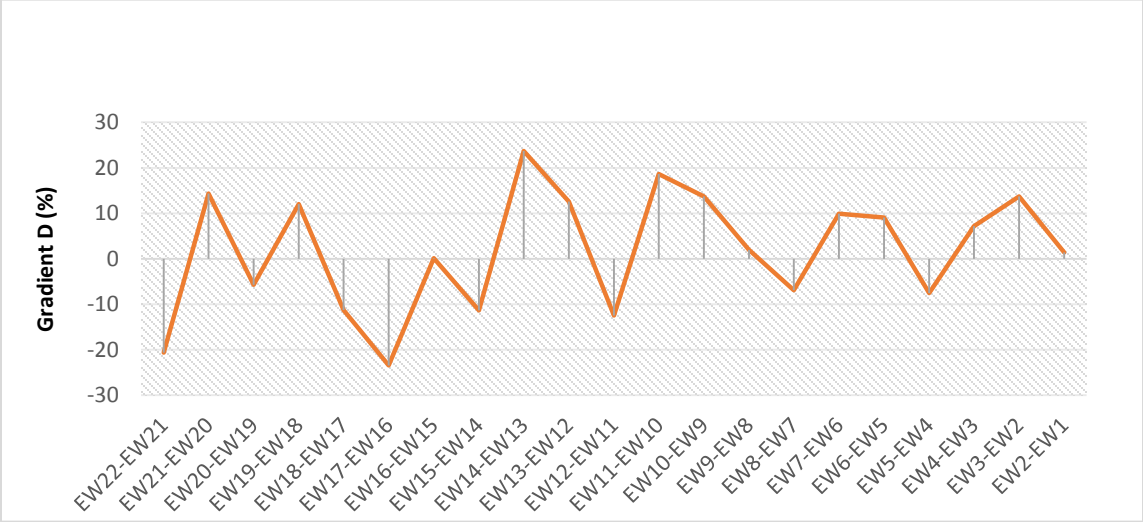

Figure 3.3 Gradient Distribution on East-West LRT Line

From the above graphs it is shown the that high gradient (steepest) on

- North-South line is 53.2 between NS23(Sebategna) - NS22(Abinet)
- East-West line is 23.7 between EW14 (Bambis) - EW13 (St.Urael).

The maximum gradient difference between two stations in AA-LRT lines is D=53.2, which is found in the stations between NS23 & NS22 and force of gradient calculated as follows.

$$F_g = 9.81WD \quad Newtons$$

Where $D = 53.2, , W = 63.3\ tonne\ F_g = 9.81 * 63.03 * \ 53.2 \qquad Newtons$

$$F_g = 32894.85 \qquad Newtons$$

c. Curve resistance:

The curve resistance force is directly proportional to the weight of the train and inversely proportional to Curve radius i.e. the small curve radius have the big curve resistance. The maximum curve radius between stations of AA-LRT is shown in the figure below.

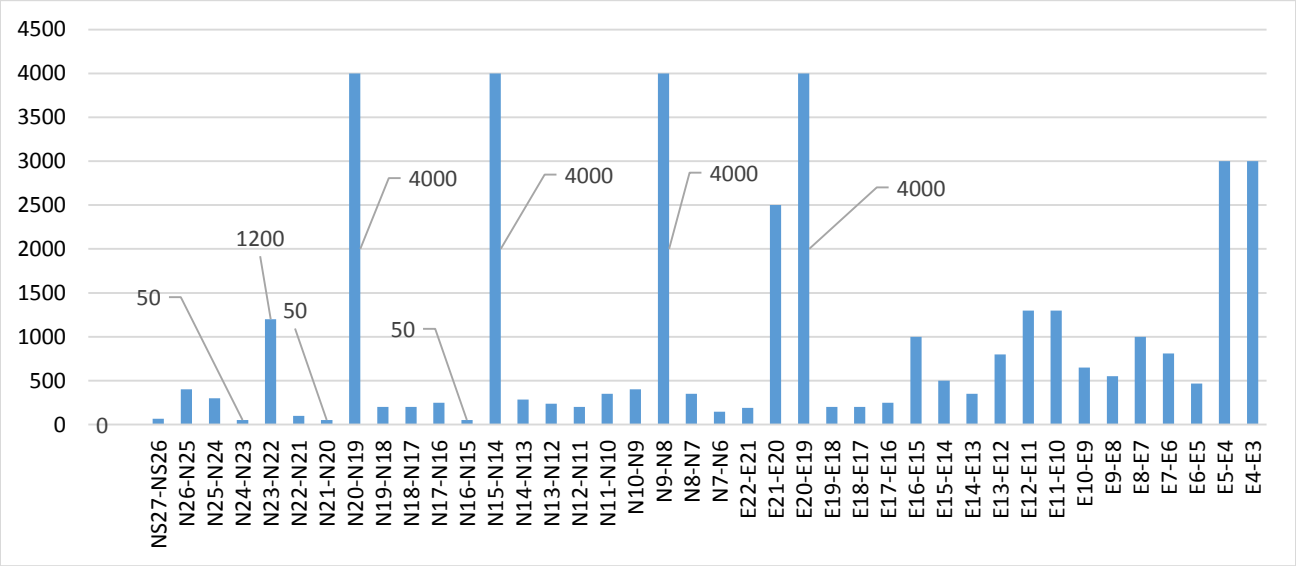

Figure 3.4 Curve Radius between Stations in AA-LRT

As Figure 3.4 shows, the curve radius between stations is in range of 50 meter to 4000 meter. But to calculate curve resistance the line NS23 (Sebategna) - NS22 (Abinet) will be used since it was selected in calculating gradient force.

$$F_c = \frac{6.5\ W}{R - 55} \qquad Newtons$$

Where: $W = 63.03\ Tonne\ , R = 1200\ meters$

$$F_c = \frac{6.5 * 63.03}{1200 - 55} \quad Newtons$$

$$F_c = \frac{6.5 * 63030}{1200 - 55} \quad Newtons$$

$$\boldsymbol{F_c = 357.8 \ \ Newtons}$$

d. Acceleration /Deceleration

The acceleration/deceleration force will exist when there is positive or negative speed change in the train, deceleration rate is the crucial variable which decide braking time and distance. To avoid wheel lockup and sliding on the rails the deceleration rate is limited to some value. In case of AA-LRT the average deceleration of vehicles under seating capacity, on rated supply voltage, on straight, dry track and with half-worn wheels will be expressed as follows:

Average deceleration for service brake

$$d = \frac{1.1m}{s^2} = 3.96 \frac{km}{hrsecond}$$

Average deceleration for emergency brake:

$$d = \frac{2\ m}{s^2} = 7.2 \frac{km}{hrs}$$

For calculating the deceleration force maximum allowable service brake is taken,

$$d = 3.96 \frac{km}{hrsecond}$$

$$F_a = 277.8\ m_e * d \quad Newtons$$

$$where;\ m_e = 1.1m\ tons = 1.1 * 63.03\ tons = 69.33\ tons$$

$$F_a = 277.8 * 69.33 * 3.96 \ \ Newtons$$

$$F_a = 76272.4\ Newtons$$

3.1.2 Braking Force

The total maximum braking force required from both electrical and mechanical brakes to stop the train in service braking time

$$F_{rb} = -(F_a + F_r + F_g + F_c) \quad Newtons$$

$$F_{rb} = -(76272.4 + 3179.6 + 32894.85 + 357.8) \quad Newtons$$

$$F_{rb} = -(112704.68) \qquad Newtons$$

$$F_{rb} = -(112.7) \qquad KN$$

But this braking force will be achieved by the four motorised wheels and two trailer wheels so the braking force required from each motorised wheel will be divided in two 6 wheel sets and on the motorised bogies the braking force achieved by both electrical and hydraulic brakes. Braking pattern used for different types of braking operations in trams used in AA-LRT shown in Table 3.1 [5].

Table 3.1 Brake Pattern for Different Braking Operations

Name	**Type**	**Mounting place**	**Service brake**	**Emergency brake**	**Safety brake**	**Stopping brake**	**Holding brake**	**Parking brake**
ED	Electric brake	M1 + M2	X	X	-	-	-	-
EHM	Hydraulic Brake of Motor Car	M1 + M2	-	X	X	X	X	X
EHT	Hydraulic Brake of Trailer Car	TB1	X	X	X	X	X	-
MTB	Magnetic track brake	M1 + M2 + TB1	-	X	X	-	-	-
Sanding	Sanding device	M1 + M2	-	X	X	-	-	-

From the above table for service braking case the braking force achieved by electrical brake and hydraulic brake (trailer bogies). There are six wheel sets on which equal braking force is applied to give optimised braking performance by avoiding unwanted longitudinal and lateral movements. The required braking force from each wheels will be

$$F_{rbW1} = \frac{F_{rb}}{6} \quad KN \tag{3.1}$$

$$F_{rbW1} = \frac{-112.7}{6} \quad KN == -18.78 \ KN$$

Braking torque of each wheel can be calculated by multiplying braking force by radius of the wheel. Diameter of the wheel is 660mm (new wheel) and 580mm (full wear), by considering the

full wear wheel the radius will be 290 mm (0.29 meter) the braking torque required from each will be

$$T_{brw1} = F_{rbw1} * r_w \tag{3.2}$$

$$T_{brw1} = -18.78KN * 0.29\ meters$$

$$T_{brw1} = -5.45\ KNm$$

Where: r_w=wheel radius in meters 0.29

The electrical motors are connected to the wheels through gear system with gear ratio of G = 8.2

$$T_{brmotor} = \frac{T_{brw1}}{G} \tag{3.3}$$

$$T_{brmotor} = \frac{-5.45\ KNm}{8.2} = -0.6659\ KNm = -665.9\ Nm$$

The above calculation is for the specific railway line between NS23 (Sebategna) - NS22 (Abinet), but it is important to calculate the braking force and torque on the other locations AA-LRT under different train weights, velocity, gradient, curve radius, gear ratio and wheel radius.

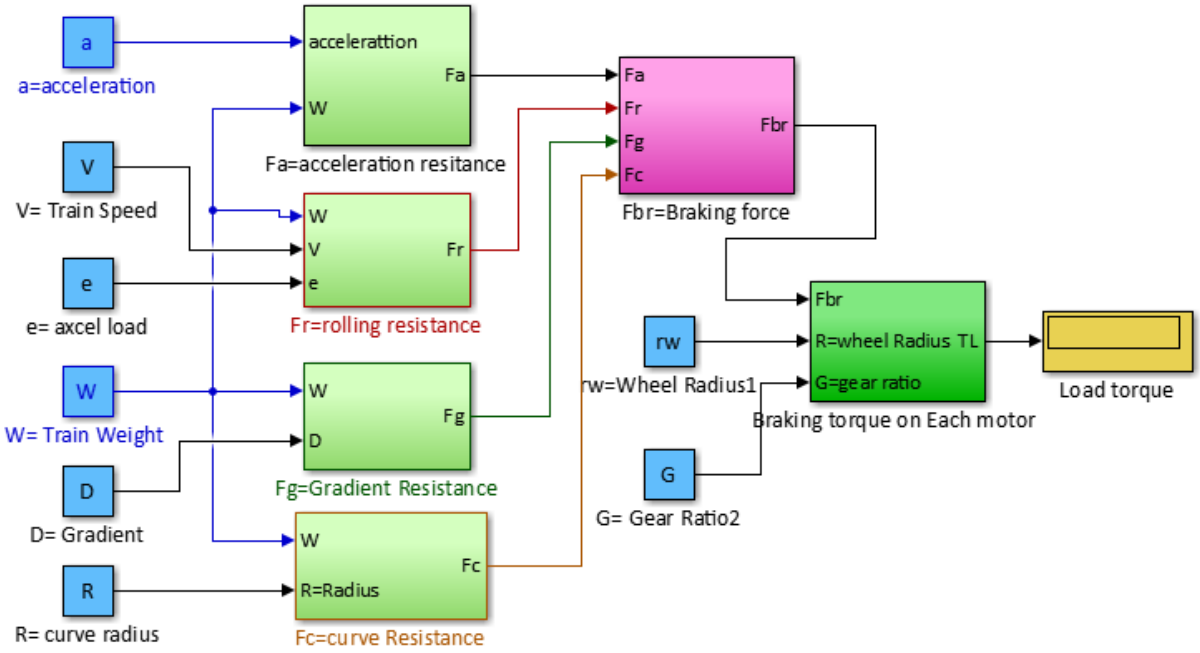

Figure 3.5 MathLab Simulink Model for Calculating Braking Torque

To solve this problem MATLAB Simulink model is developed (See Figure 3.5) for calculating braking torque, the model will take different conditions and it will calculate the different resistance forces, braking force and braking torque. By using this model braking torque required for journey between two stations will be calculated for both lines of AA-LRT

1. From station NS-27 (Minilik Square) to NS-6 (Kality) for the journey between all stations in both directions.(see the attached appendix)
2. From station EW-22 (Tor hailoch) to EW-1 (Ayat) for the journey between all stations in both directions and it will be discussed in the next chapter

3.1.3 Braking Distance and Time

Braking distance and time can be determined from acceleration and initial velocity of the train. Speed time graph shows how station to station speed trajectory determines the time taken for acceleration, constant speed and deceleration as shown in the Figure 3.6 below.

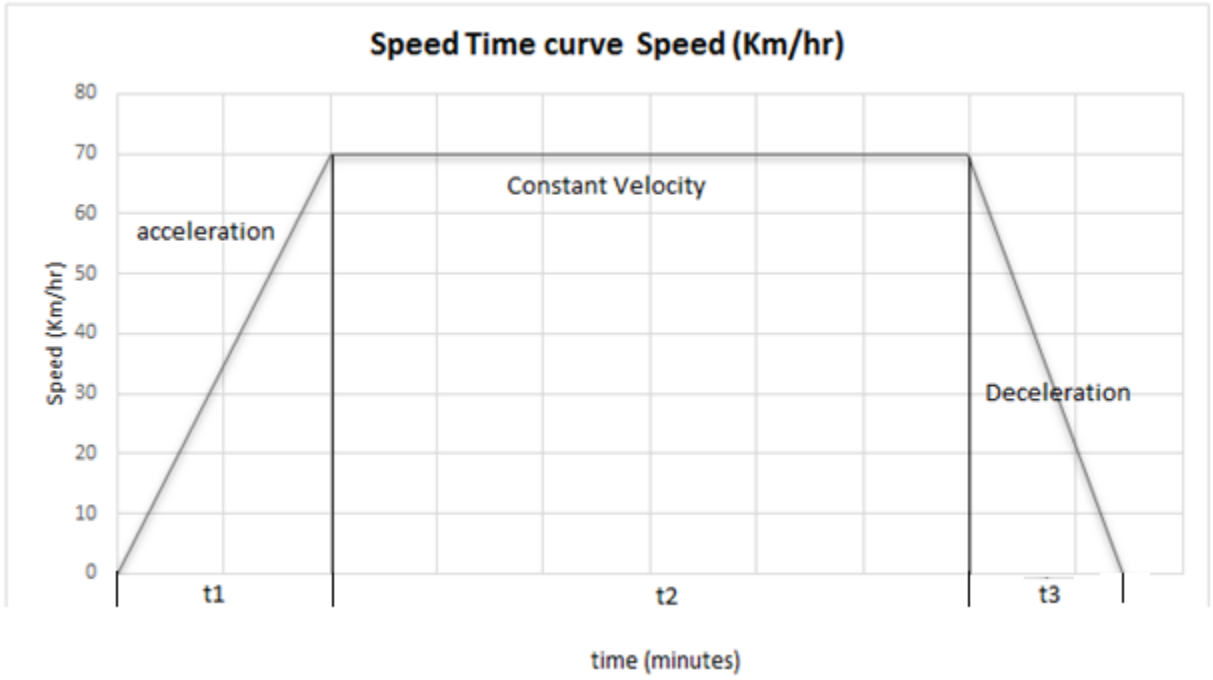

Figure 3.6 Speed Time Curve for Urban Trams

In urban areas the coasting deceleration distance is almost zero since the distance between two stations is short and it is excluded from the speed time curve as shown in Figure 3.6, we can calculate the value of t_1, t2 and t_3 and the corresponding distance covered.

Calculating time required for acceleration

$$t_1 = \frac{V_f - V_i}{a} \qquad (3.4)$$

$$t_1 = \frac{70kmph - 0kmph}{3.24kmphps}$$

$$t_1 = 21.61\ Seconds$$

$$t_1 = 0.36\ minutes$$

$$S_1 = \frac{1}{2} * (V * t_1) \qquad (3.5)$$

$$S_1 = \frac{1}{2} * (70kmph * (\frac{0.36}{60} h))$$

$$S_1 = \frac{1}{2} * (70kmph * (\frac{0.36}{60} h))$$

$$S_1 = 0.21km$$

Calculating time required for deceleration

$$t_3 = \frac{V_f - V_i}{d}$$

$$t_3 = \frac{0kmph - 70kmph}{-3.96kmphps}$$

$$t_3 = 17.677\ seconds$$

$$t_3 = 0.295\ minutes$$

$$S_3 = \frac{1}{2} * (V * t_3)$$

$$S_3 = \frac{1}{2} * (70kmph * (\frac{0.295}{60} h))$$

$$S_3 = 0.172\ km$$

Train braking distance depends on:-deceleration rate, train speed, traction weight, braking technology and signal block system.

Constant velocity running time depends on distance between two stations, the distance between stations NS23 and NS22 is 0.861 km. From this length constant velocity running time can be calculated as follows.

$$S_2 = S - (S_1 + S_3) \qquad (3.6)$$

$$S_2 = 0.861 - (0.21 + 0.172)km$$

$$S_2 = 0.479\ km$$

$$t_2 = \frac{S_2}{V_m}\ minutes \qquad (3.7)$$

$$t_2 = \frac{0.479}{70} * 60\ minutes$$

$$t_2 = 0.411\ minutes$$

$$t_{total} = t_1 + t_2 + t_3 \qquad (3.8)$$

$$t_{total} = 0.36 + 0.411 + 0.172$$

$$t_{total} = 0.943\ minutes$$

Where

V_i= Initial velocity

V_f= Final velocity

a= Acceleration

d= Deceleration

t_1= Acceleration time

S_1= Acceleration distance

t_2=Constant speed running time

S_2= Constant speed running distance

t_3=Ceceleration time

S_2= Deceleration distance

t=Total time

S= Total distance b/n stations

Figure 3.7 shows that the time taken for decelerating train will be varied based on the deceleration rate, it is clear that the braking time and distance are dependent on the deceleration rate.

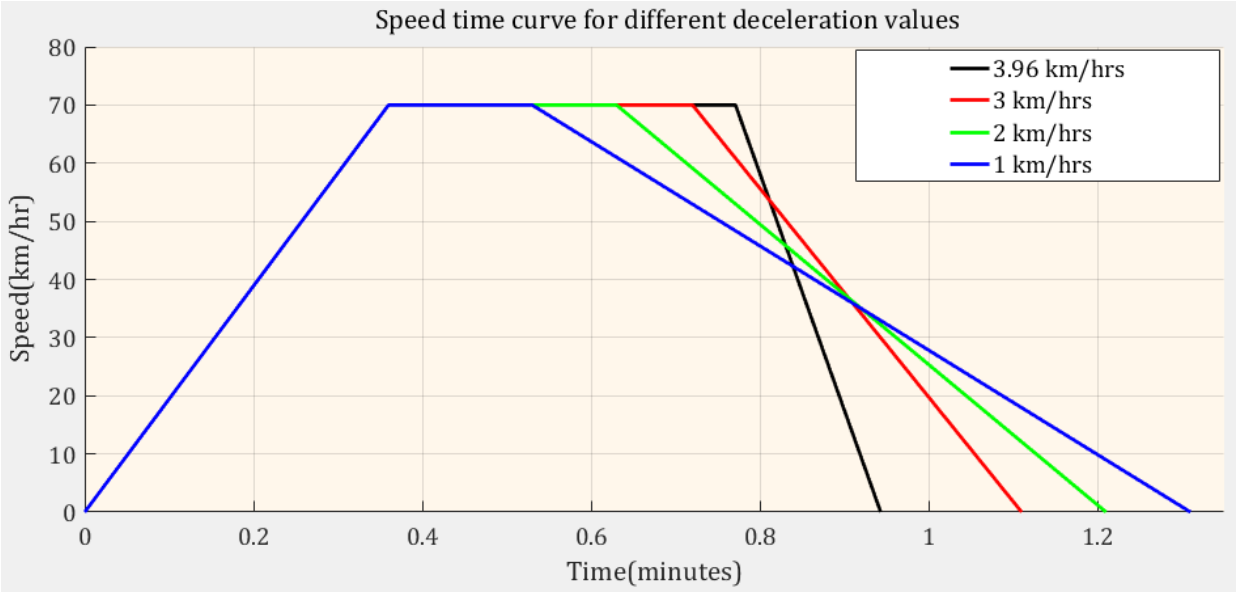

Figure 3.7 Speed Time Curve for Different Deceleration Values

3.2 Electrical Traction and Braking System Modelling

Generally electrical traction and braking system includes traction inverter, braking controller, brake resistor and traction motors as key electrical equipment, moreover, as high voltage electric equipment such as pantograph, main circuit breaker and surge arrestor. Train shall be equipped with two motor bogies and one trailer bogie, so that each traction inverter shall be able to power the two traction motors on one bogie. In this section traction inverter, traction motor and braking controller are modelled.

3.2.1 Traction Power Converter Modelling

CNE PW-260/D/H-02 is traction converter cabinet contains 2 sets of 130 KW traction converter units, which are used to provide variable frequency, variable voltage power supply to the traction motor of the light rail vehicle and for auxiliary power supply for utilisation systems inside the cabin [22].

Traction inverter mainly consists of line contactor, IGBT switching bridge, chopper power unit, logic control unit and filter capacitor. The function of three phase inverter is basically to convert the DC voltage fed from the pantograph in to AC voltage with amplitude and frequency determined by motor speed controller (variable speed, variable frequency drive).

The rated supply voltage of the main circuit of the converter is DC 750V; the output voltage of the traction inverter in traction mode is 0-510V, and the frequency is 0-185Hz; the output voltage of the traction inverter in braking mode is 0-598V, the frequency is 0-185Hz.

The traction inverter can feed the braking energy back to the grid through the DC input link in brake condition. When there is no other light rail vehicle working in the power grid to absorb its braking energy, this energy will be absorbed by the braking resistor.

The traction inverter adopts the control strategy of the advanced Proportional and Integral based VVVF control, and the changes of electrical parameters of the motor impose very little influence on the control characteristics. The VVVF control has advantages of good output characteristics and it needs relatively simple control system.

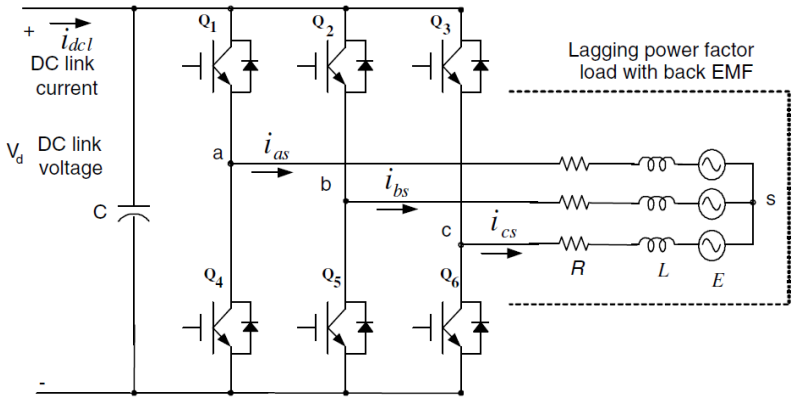

Figure 3.8 IGBT Based Voltage Source Inverter Supplied Induction Motor [34]

The Variable Voltage Variable Frequency (VVVF) inverter with Pulse Width Modulation (PWM) technology is utilized to control the train speed. The drive system uses a six pulse inverter with a high switching frequency device, Insulated Gate Bipolar Transistor (IGBT). With the high switching speeds and advanced PWM schemes, the performance of an inverter is significantly improved in terms of odd harmonics rejection.

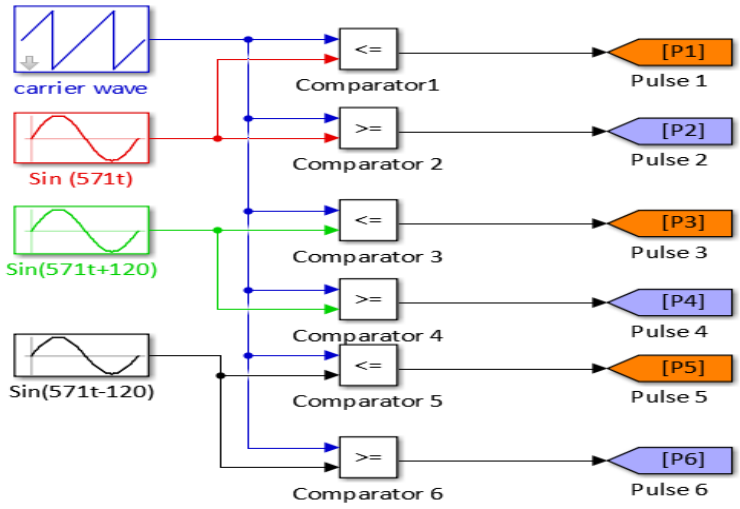

Figure 3.9 Pulse Width Modulation for Inverter Switching

The sinusoidal PWM uses a carrier comparison scheme to produce the gate signals of the inverter. To obtain a balanced three phase output voltages, the saw tooth voltage waveform (carrier wave Vc, frequency of 4kHz) is compared with three sinusoidal control voltages (reference wave Vr, frequency fr) that are 120 degrees out of phase.

The intersection of Vc and Vr waves determines the switching instants and commutation of the modulated pulse. The carrier and reference waves are mixed in a comparator. When sinusoidal wave has magnitude higher than the saw tooth wave, the comparator output is high (Vdc), otherwise it is low (-Vdc). The Figure 3.9 shows the simulation circuit of PWM in MATLAB.

The ratio of Vr / Vc is called the modulation index (MI) and it controls the harmonic content of the output voltage waveform. The magnitude of fundamental component of output voltage is proportional to MI when MI is less than one. Thus the output voltage is controlled by varying MI. Frequency of the output wave is the same as frequency of the reference sinusoidal wave. The LRT tramcar induction motor has a rating of 130KW, 500V and 91Hz. The magnitude of the MI for six pulse inverter is calculated using the next formula [37].

$$V_{ab} = \frac{V_{motor}}{\sqrt{3}}\sqrt{2} \tag{3.9}$$

$$V_{ab} = \frac{500V}{\sqrt{3}}\sqrt{2} = 408\ V$$

Giving tolerance for the voltage transient 50%

$$V_{abpeak} = 408V * 1.5 = 612V \tag{3.10}$$

DC link voltage $V_{dc} = 750\ V$

Therefor

$$MI_{max} = \frac{V_{abpeak}}{V_{dc}} = \frac{612V}{750V} = 0.82 \tag{3.11}$$

Where V_{motor} = phase to phase rms voltage of stator winding

V_{ab} = phase to phase rms voltage of inverter

$V_{ab\ peak}$ = maximum phase to phase rms voltage of inverter

V_{dc} = dc input voltage of inverter

MI = modulation index

From the Sinusoidal PWM, the modulation index is the ratio of amplitude of the reference voltage to the amplitude of the saw tooth wave. By assuming the amplitude saw tooth wave equal to unity, the amplitude reference waves of the can be calculated as;

$$V_r = \frac{V_c}{MI} = \frac{1}{0.82} = 1.22 \tag{3.12}$$

The comparator compares the magnitude of the sinusoidal and the saw tooth waves and outputs one if sinusoidal wave is higher than saw tooth wave otherwise outputs zero.

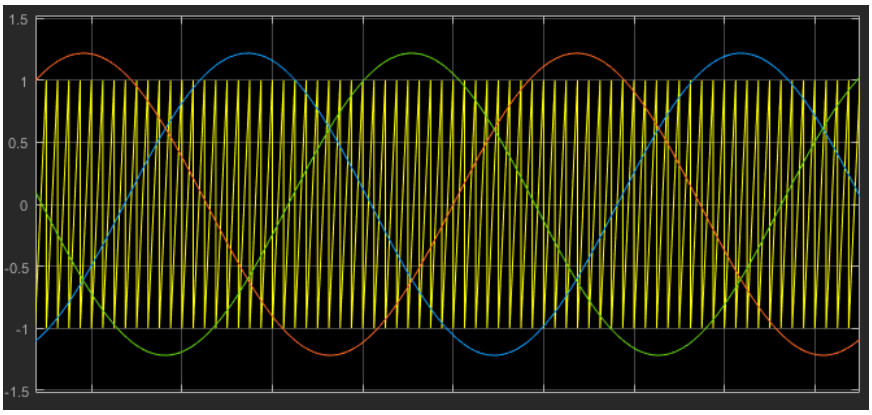

Figure 3.10 Comparator Input, Sinusoidal and Triangular Wave

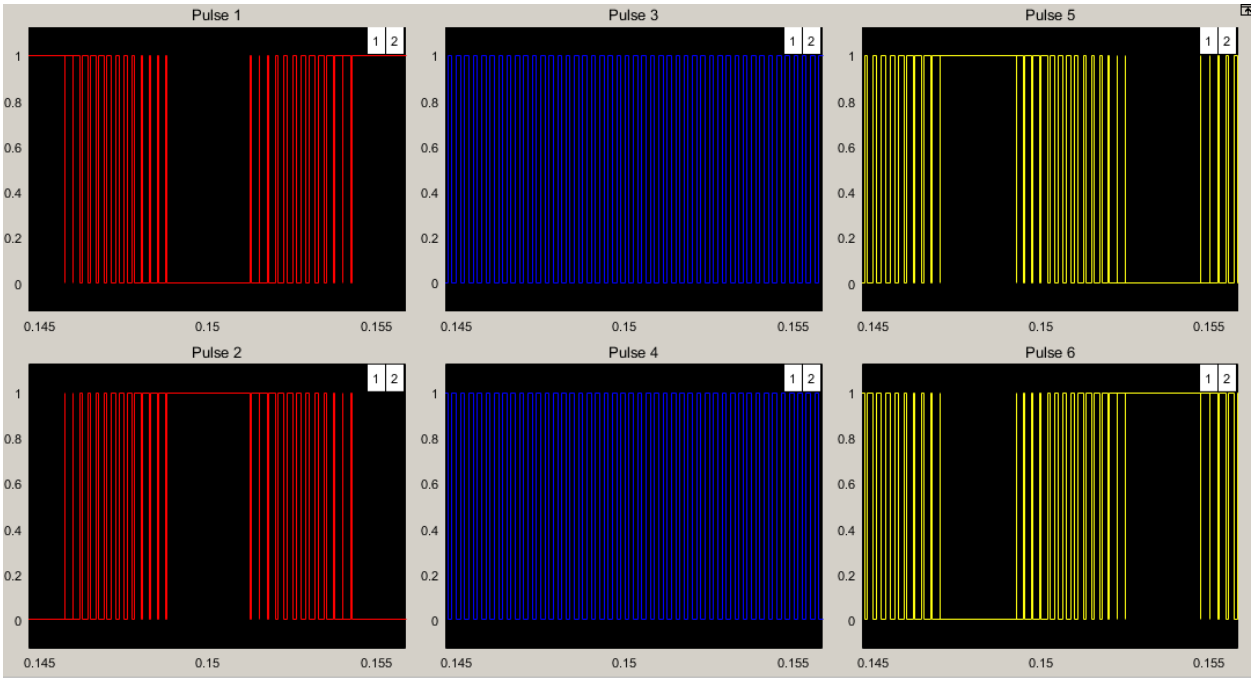

Figure 3.11 VVVF Inverter Gate Trigger Pulses

3.2.2 Traction Motor Modelling

YJ128C asynchronous traction motor equipped on 70% low-floor vehicle is supplied by voltage source inverter which is used in AA-LRT. Traction motor employed 3-phase squirrel cage asynchronous traction motor, and cooled by self-ventilation.

Traction motor is utilized for vehicle traction and braking. Motoring is supplied by traction inverter. Traction motor drives the axles through gear transmission unit. Braking is supplied by traction motor. Energy is fed back to power network through brake chopper module (regenerative braking) or such energy is depleted by brake resistor (resistance braking).

Table 3.2 Specifications of Traction Motor

Parameter	Value	Parameter	Value
Rated power	130KW	Rated efficiency	0.924
Rated voltage	500V	Weight	440±3%kg
Rated current	215A	Rs (stator coil resistance)	0.1968 ohms
Rated frequency	91Hz	Ls (stator coil inductance)	0.00182 henry
No of Poles	6	Xs(stator coil reactance)	0.10400936 ohms
Rated rotating speed	1800r/min	Rr'(rotor coil resistance)	0.164 ohms
Rated rotating speed	188.4 rad/s	Lr'(rotor coil inductance)	0.00152 henry
Synchronous Speed	1820r/min	Xr (rotor coil reactance)	0.08686496 ohms
Synchronous Speed	190.5 rad/sec	Lm(core inductance)	0.001599henry
Rated torque	689N·m		

By using equation 3.21 the employed motor torque speed characteristics curve plotted on MathLab.

$$T_m = 3\frac{P}{2}\frac{r_r}{\omega s}\frac{(V_1)^2}{\left(\frac{r_r}{s}+r_s\right)^2+(\omega L_s+wL_r)^2}$$

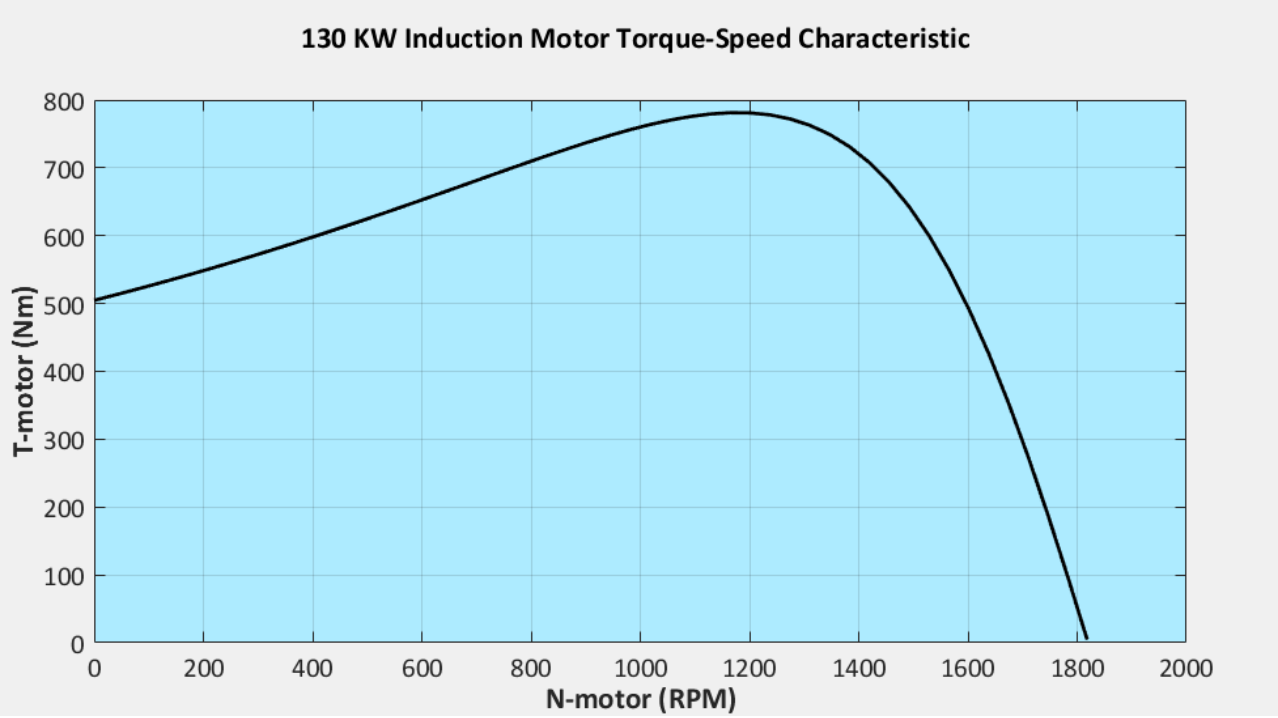

Figure 3.12 Torque Speed Characteristics of 130 KW Induction Motor

By considering AA-LRT traction system data MathLab Simulink model of induction motor and traction inverter is developed as shown on Figure 3.13.

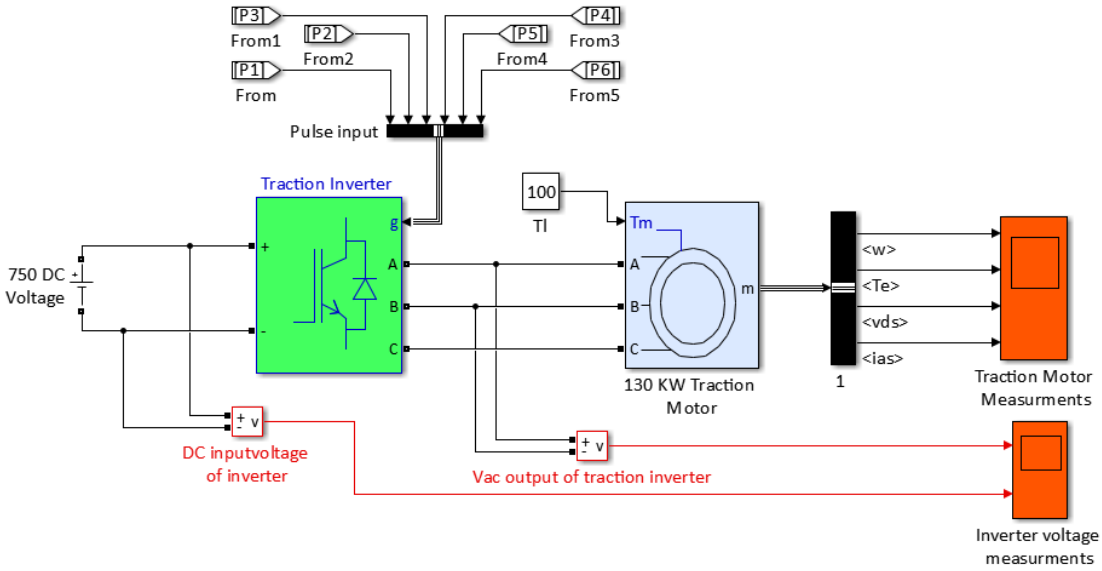

Figure 3.13 Modelling of Inverter Fed 130 KW Induction Motor

Applying the pulse width modulated gate signal to the IGBT switch, we get a sinusoidal voltage with its harmonic contents (see Figure 3.13). Based on the basic power electronic principle, voltage output of the voltage source inverter (VSI) depends on the switching character, whereas the output current depends on the output load. As the load impedance seen from the converter is inductive reactance, the current looks more sinusoidal than the voltage.

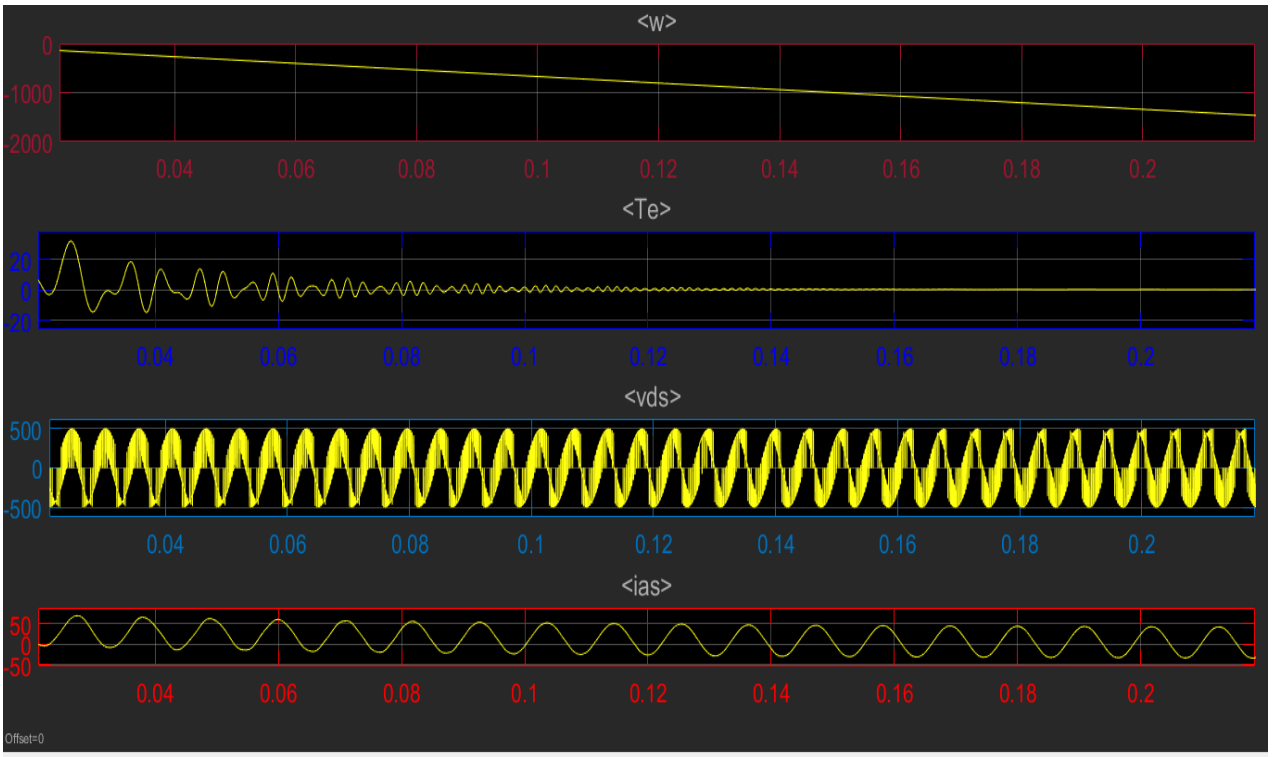

Figure 3.13 Characteristics 130 KW Induction Motor

Applying 750 dc-link voltage and 0.8 modulating index and negative constant load (to model the braking mode) the transient response looks like the one shown in Figure 3.13. The electrical torque settles to zero steady state value after oscillating for tenth of a second while the speed goes to negative value the steady state value because of the applied negative load to simulate the braking mode.

3.2.3 PI Based VVVF Speed Controller

The basis of constant V/F speed control of induction motor is to apply a variable magnitude and variable frequency voltage to the motor (Figure 3.14). The following block diagram shows the closed loop V/F control using a VSI.

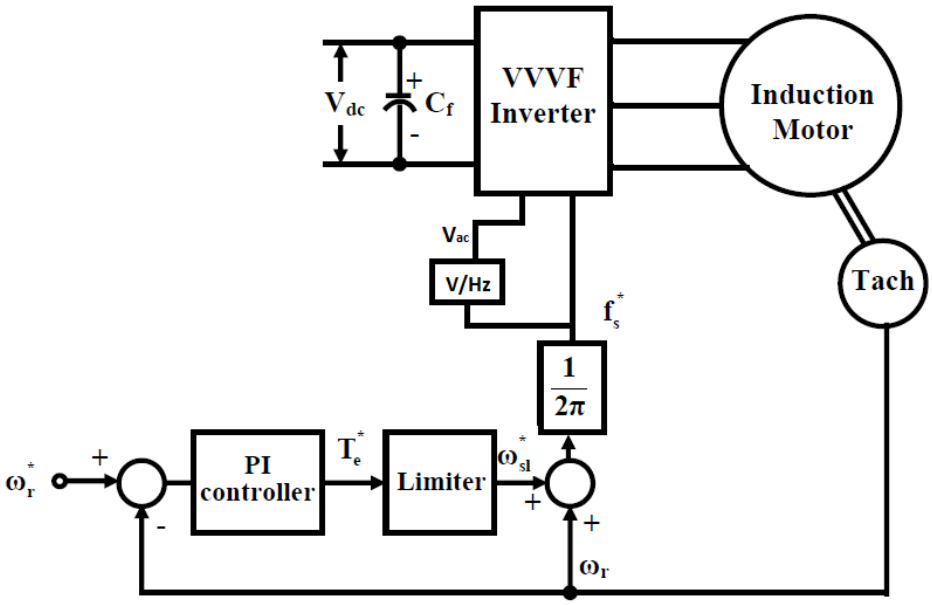

Figure 3.14 Closed-Loop V/Hz Constant Control [26]

The closed-loop method offers a more precise solution to controlling the speed. Furthermore, the closed-loop technique controls the torque, too. The desired torque is only accessible at the nominal operating point. If the load torque changes, the speed will be kept constant at the set point the motor will change [38].

3.3 Modelling of PI Controlled Plant

The most commonly used controller for the speed control of Induction motor is PI controller. The combination of proportional and integral terms is important to increase the speed of the response and also to eliminate the steady state error. To model the existing traction and braking control system let us consider quarter model of the rolling stocks. The dynamics of the rolling stocks are simplified by using a quarter model, which is based on the assumption that the rolling stocks travel in the longitudinal direction without lateral motion [39].

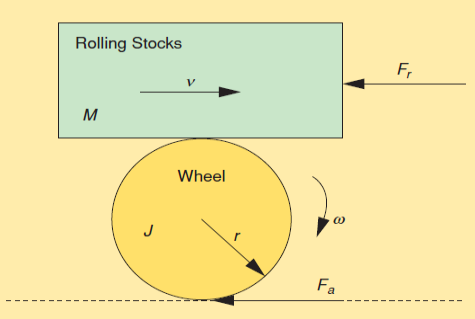

Figure 3.15 Quarter Model of the Rolling Stocks [39]

The equations of motion for the quarter model of the rolling stocks can be expressed as

$$J\dot{\omega} = -B\omega + T_a - T_L - T_d \tag{3.13}$$

where B is the viscous friction torque coefficient between the brake pad and the wheel; Ta = input torque and T_L=load torque, respectively; Td is the disturbance torque due to the vibration of the brake caliper; J and r are the inertia and radius, respectively, of each wheel of the rolling stocks.

Taking the Laplace transform of Equation (3.22)

$$T_a - T_L - T_d = \frac{1}{Js + B} \tag{3.14}$$

By using the above equation as a plant model the PI controller including load torque and induction motor is modeled simply in MathLab as shown in the in Figure 3.16 below.

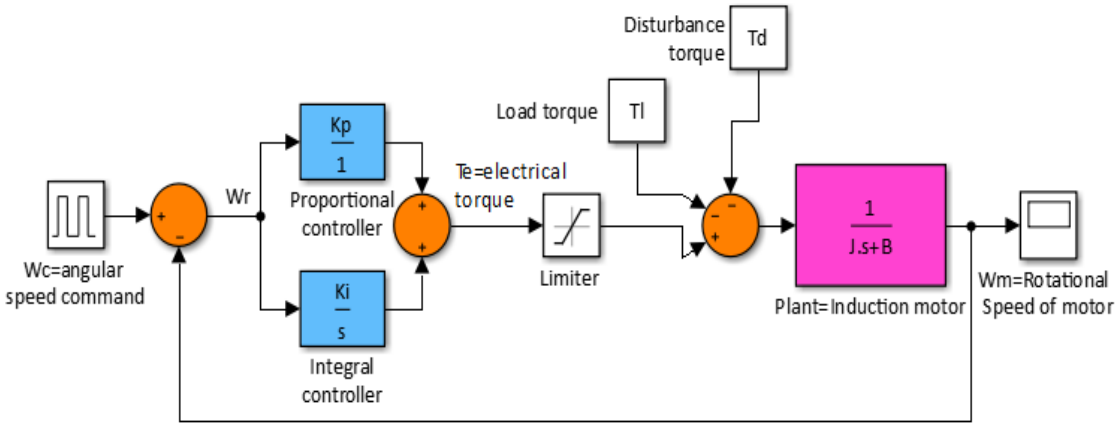

Figure 3.16 MathLab Simulink Model for PI Controller

The closed loop transfer function of the system will became for zero load and disturbance force

$$\frac{W_m(s)}{W_c(s)} = \frac{\left(\frac{1}{J}\left(K_p s + K_i\right)\right)}{s^2 + s\left(\frac{B}{J} + \frac{1}{J}K_p\right) + \frac{1}{J}K_i} \tag{3.15}$$

If we consider a denominator of standard second-order transfer function with natural frequency ω_n and damping ratio ξ , then changing the denominator of the above transfer function to the standard[36].

$$d(s) = s^2 + 2\omega_n\,\xi + \omega_n^2 = s^2 + s\left(\frac{B}{J} + \frac{1}{J}K_p\right) + \frac{1}{J}K_i \tag{3.16}$$

$$K_i = J\omega_n^2\,, K_p = (2\omega_n\,\xi * J) - B \tag{3.17}$$

ω_n can be found from the band width of the controller by using

$$\omega_n = 2\pi\, BW \tag{3.18}$$

And BW of a closed loop speed controller will dependent of switching frequency of the inverter and ξ can be taken 0.71 the bandwidth BW will be 1 HZ [35].

$$\omega_n = 2\pi\, BW = 2\pi * 1 = 6.283$$

$$\xi = 0.71$$

From the traction motor parameters

B (viscous friction torque coefficient) = 0.005 N-m-s, J (Motor shaft inertia) = 0.089 Kg-m^2

Now it is possible to find proportional and integral gains by using equation 3.26

$$K_p = (2\omega_n\,\xi * J) - B = (2 * 6.283 * 0.71 * 0.089) - 0.005$$

$$K_p = 0.789$$

$$K_i = J\omega_n^2 = 0.089 * (\,6.283)^2 = \;3.513$$

After putting the numerical values to the MathLab Simulink model, the model will look like as shown in Figure 3.17.

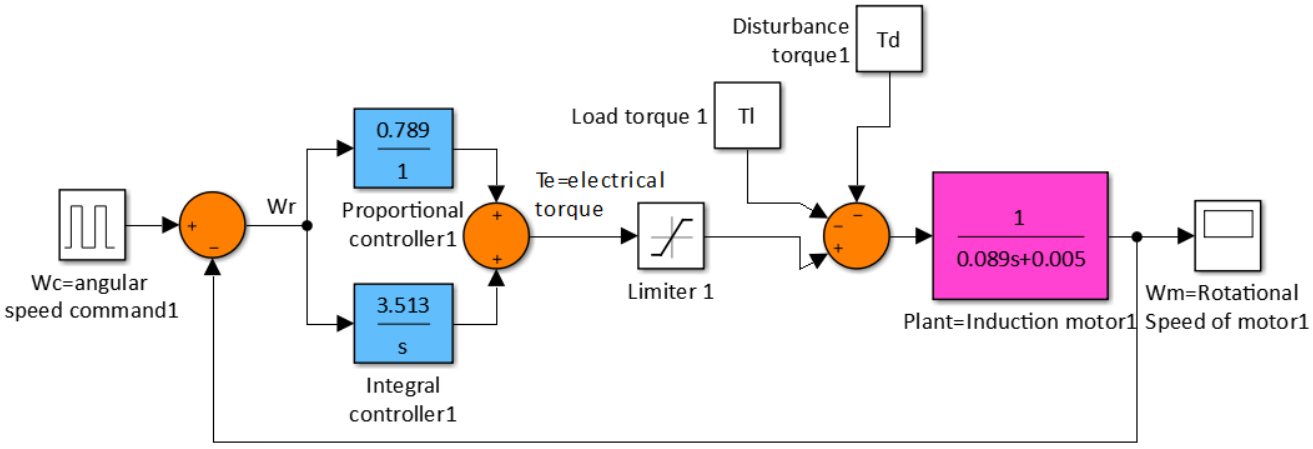

Figure 3.17 MathLab Simulink Model for PI Controller with Actual Data

The speed loop error generates the slip speed command Wr then through the proportional–integral controller (PI) the required electrical torque will be generated to achieve the set point speed by overcoming load and disturbance torques. [40].

A step increase in speed command W_C produces a positive speed error Wr is set at the maximum value. The drive accelerates at the permissible current, producing the maximum available torque, until the speed error is reduced to a very small value or zero theoretically.

A step decrease in speed command W_c produces a negative speed error. Wr is set at the maximum negative value. The drive accelerates under regenerative braking; at the maximum permissible current and the maximum available braking torque, until the speed error is reduced to a small value. Now the operation shifts to generating mode and the drive settles at the set point speed for which the motor torque equal the demand torque.

On MathLab Simulink the system response for different reference conditions will be simulated and compared with the developed adaptive controlled in the next chapter.

3.4 Development of Model Reference Adaptive Controller

Torque is the fundamental variable of an induction machine, to get the accurate control of speed is by controlling the torque of induction machines in braking operation under disturbance and load torque. However, the PI controller has poor transient response because of the negative zero on the actual transfer function, such as the high starting overshoot, sensitivity to controller gains and sluggish response due to sudden disturbance. So, it is important to develop a new Adaptive controller by using MathLab/Simulink package which will give better responses than the traditional PI controller for the speed control. AS it was discussed in the previous chapter for this thesis work Model Reference Adaptive Controller (MRAC) will be used and the adaptation mechanism will be based on MIT rule.

The adaptive control theory provides an approach to design of uncertain systems. Unlike the fixed parameter controller the adaptive controller adjust its behavior on-line to the changing property of the controlled processes. The main difference between the conventional control and adaptive control is the presence of adaption mechanism. The main issue in adaptation design is to synthesize an adaption mechanism which will guarantee that the control system remains robust.

The MRAC is a reference model based adaptive control system in which the adjustment mechanism is designed using MIT rule. The block diagram of MRAC is shown in Figure 3.18.

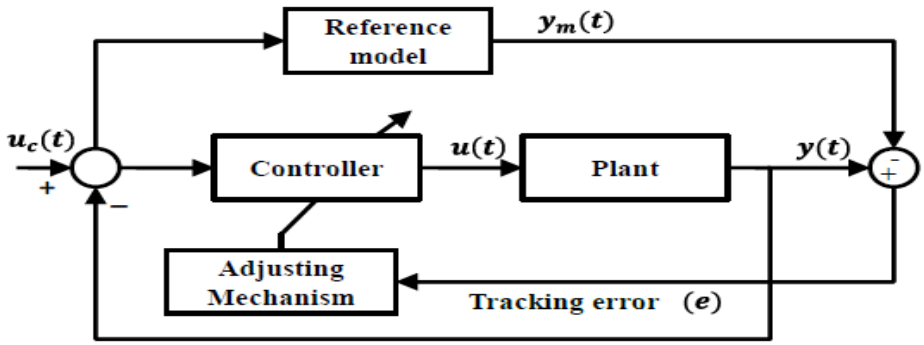

Figure 3.18 Block Diagram of Model Reference Adaptive Control [40]

As it is shown in the picture MRAC system consists of 4 main components:

1. Plant to be controlled
2. Reference model to generate desired closed loop output response

3. Controller that is time-varying and whose coefficients are adjusted by adaptive mechanism
4. Adaptive mechanism that uses 'error' (the difference between the plant and the desired model output) to produce controller coefficient.

3.4.1 Plant Model to be Controlled

The transfer function of the plant (induction motor) can be expressed as the same way as PI plant model by using speed of the motor $\omega_m(s)$ as output and control and set point speed $\omega_c(s)$ as input for the controller.

$$\frac{y(s)}{u_c(s)} = \frac{b}{s+a} = \frac{W_m(s)}{W_c(s)} = \frac{1}{JS+B} \tag{3.19}$$

After introduction of the PI controller to the plant the structure becomes

$$\frac{y(s)}{u_c(s)} = \frac{b(k_p s + K_i)}{s^2 + s(a + bk_p) + bk_i} \tag{3.20}$$

$where: b = \frac{1}{J} \quad and\ a = \frac{B}{J}$

$$\frac{W_m(s)}{W_c(s)} = \frac{\left(\frac{1}{J}(K_p s + K_i)\right)}{s^2 + s\left(\frac{B}{J} + \frac{1}{J}K_p\right) + \frac{1}{J}K_i} \tag{3.21}$$

Closed loop transfer function of the system will became

$$\frac{W_m(s)}{W_c(s)} = \frac{K_p s + K_i}{Js^2 + s(B + K_p) + K_i}$$

Where

$y(s)$=Plant output

$W_c\ (s)$=Speed command

$u_c\ (s)$= Command signal

J= Motor shaft inertia

$W_m(s)$= actual speed of motor

B= Viscous friction torque coefficient

K_p=Proportional gain $a\ and\ b$= coefficients

K_i=Integral gain

3.4.2 Reference Model

According to the closed loop transfer function of the system with PI controller the reference model will be

$$\frac{y_m(s)}{u_c(s)} = \frac{W_{model}}{W_c} = \frac{b_{m1}s + b_{m2}}{s^2 + a_{m1}s + a_{m2}}$$

$$a_{m1} = b_{m1} = a + bK_p$$

$$a_{m1} = b_{m1} = \frac{B}{J} + \frac{K_p}{J} = \frac{B + K_p}{j}$$

$$a_{m2} = b_{m2} = bk_i = \frac{k_i}{J} \qquad (3.22)$$

Replacing a_m and b_m variables by controller gains and motor parameters.

$$\frac{y_m(s)}{u_c(s)} = \frac{W_{model}}{W_c} = \frac{b_{m1}s + b_{m2}}{s^2 + a_{m1}s + a_{m2}}$$

$$\frac{W_{model}}{W_c} = \frac{(K_p + B)s + Ki}{Js^2 + (K_p + B)s + Ki}$$

Where

$W_{model}(s)$= Speed output from the reference model

$a_{m1}, a_{m2}, b_{m1}, b_{m2}$= coefficients

3.4.3 Adaptation Mechanism

Adaptation in MRAC makes an adjustment of some or all of the controller coefficients so as to force the response of closed-loop control system similar to the input command. In this case both proportional and integral gains will be modified by the adaptation loop.

For the proportional gain the adaptation mechanism will be calculated

$$\frac{dK_p}{dt} = -\gamma_p^l e \frac{a_{m1}s}{(s^2 + sa_{m1} + a_{m2})}(u_c - y)$$

From section 3.4.2 the variables are defined as follows

$$where\ ; \qquad e = W_m - W_{model} \tag{3.23}$$

$$u_c - y = W_c - W_m \tag{3.24}$$

$$a_{m1} = b_{m1} = \frac{B}{J} + \frac{K_p}{J} = \frac{B + K_p}{j}$$

$$a_{m2} = \frac{k_i}{J}$$

$$\gamma_p^l = \frac{\gamma_p b}{a_{m1}}$$

$$\frac{dK_p}{dt} = -\gamma_p(W_m - W_{model}) * \frac{s}{\left(Js^2 + s\left(B + k_p\right) + K_i\right)}(W_c - W_m) \tag{3.25}$$

For the integral gain adaptation mechanism will be

$$\frac{dK_i}{dt} = -\gamma_i^l e \frac{a_{m1}}{\left(s^2 + s\left(a + bk_p\right) + bk_i\right)}(u_c - y)$$

$$\frac{dK_i}{dt} = -\gamma_i(W_m - W_{model}) * \frac{1}{\left(Js^2 + s\left(B + k_p\right) + K_i\right)}(W_c - W_m) \tag{3.26}$$

Where

γ_p= adaptation gain for proportional controller

γ_i= adaptation gain for integral controller

Mathematical model MRAC components is done, so now it is important to put the numerical values in to the formulas to get the final model as follows. From the previous section (modeling of PI controller) the following values are computed.

J= 0.089 Kg-m^2, B= 0.005 N-m-s

$K_p = 0.789$, $K_i = 3.513$

1. Closed Loop Transfer function of plant without PI controller

$$\frac{W_m(s)}{W_c(s)} = \frac{1}{JS + B}$$

$$\frac{W_m(s)}{W_c(s)} = \frac{1}{0.089\,S + 0.005}$$

2. Transfer function of reference model

$$\frac{W_{model}}{W_c} = \frac{(K_p + B)s + Ki}{Js^2 + (K_p + B)s + Ki}$$

$$\frac{W_{model}}{W_c} = \frac{(0.789 + 0.005)s + 3.513}{0.089s^2 + (0.789 + 0.005)s + 3.513}$$

$$\frac{W_{model}}{W_c} = \frac{0.794s + 3.513}{0.089s^2 + 0.794s + 3.513}$$

3. Transfer function of Adaptation mechanism

For proportional controller

$$\frac{dK_p}{dt} = -\gamma_p(W_m - W_{model}) * \frac{s}{\left(Js^2 + s\left(B + k_p\right) + K_i\right)}(W_c - W_m)$$

$$\frac{dK_p}{dt} = -\gamma_p(W_m - W_{model}) * \frac{s}{0.089s^2 + 0.794s + 3.513}(W_c - W_m)$$

For integral controller

$$\frac{dK_i}{dt} = -\gamma_i(W_m - W_{model}) * \frac{s}{\left(Js^2 + s\left(B + k_p\right) + K_i\right)}(W_c - W_m)$$

$$\frac{dK_i}{dt} = -\gamma_i(W_m - W_{model}) * \frac{s}{0.089s^2 + 0.794s + 3.513}(W_c - W_m)$$

γ_p= adaptation gain for proportional controller and γ_i= adaptation gain for integral controller different values will be taken to tune the adaptation system.

After modeling plant, controller and adaptation mechanism using MIT rule, MRAC system is developed in MathLab Simulink as shown in the Figure 3.19.

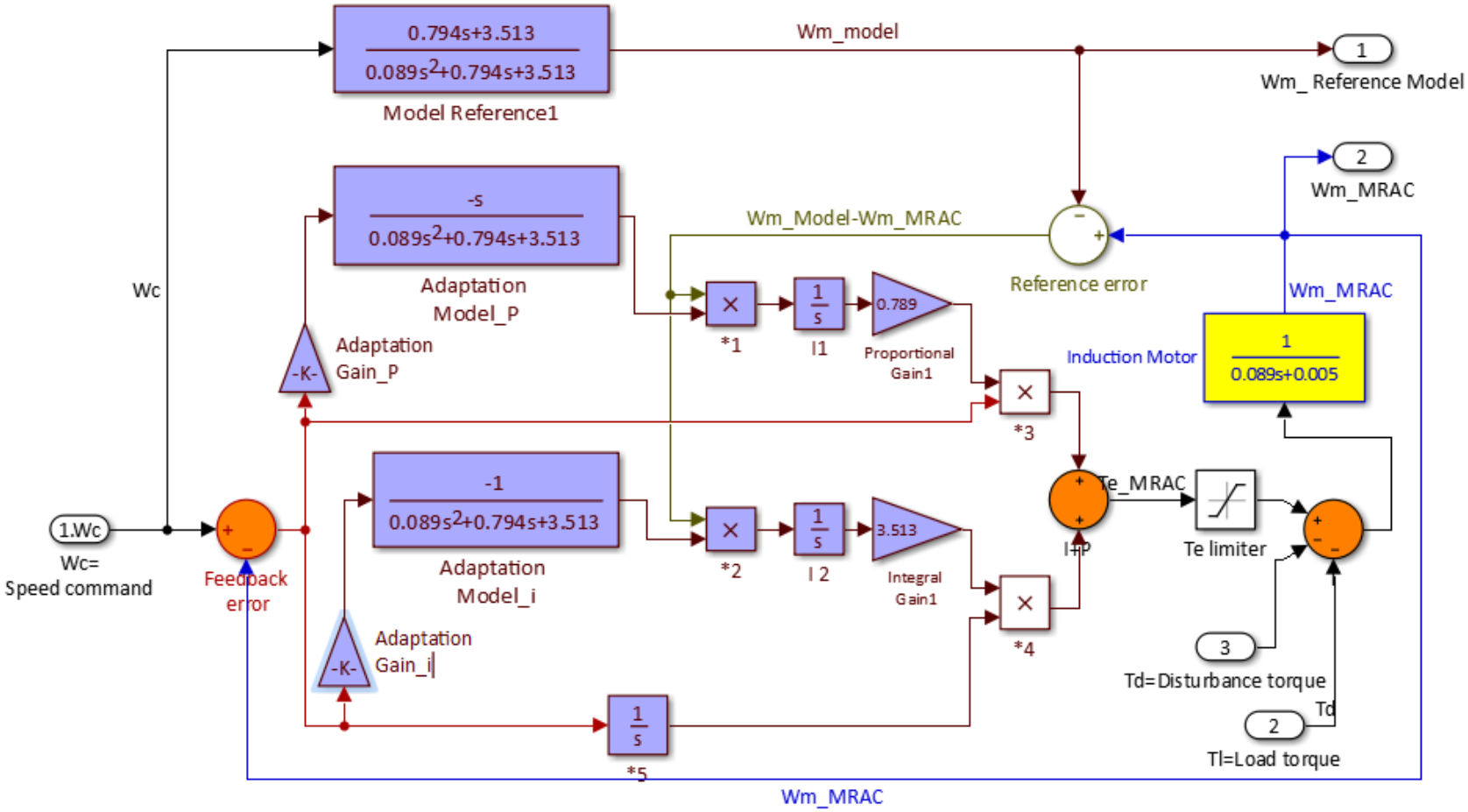

Figure 3.19 Model Reference Adaptive Controller for AA-LRT Train Braking System

For describing the designed system the model can be simplified as shown in the next picture by putting the PI + adaptation mechanism in one subsystem.

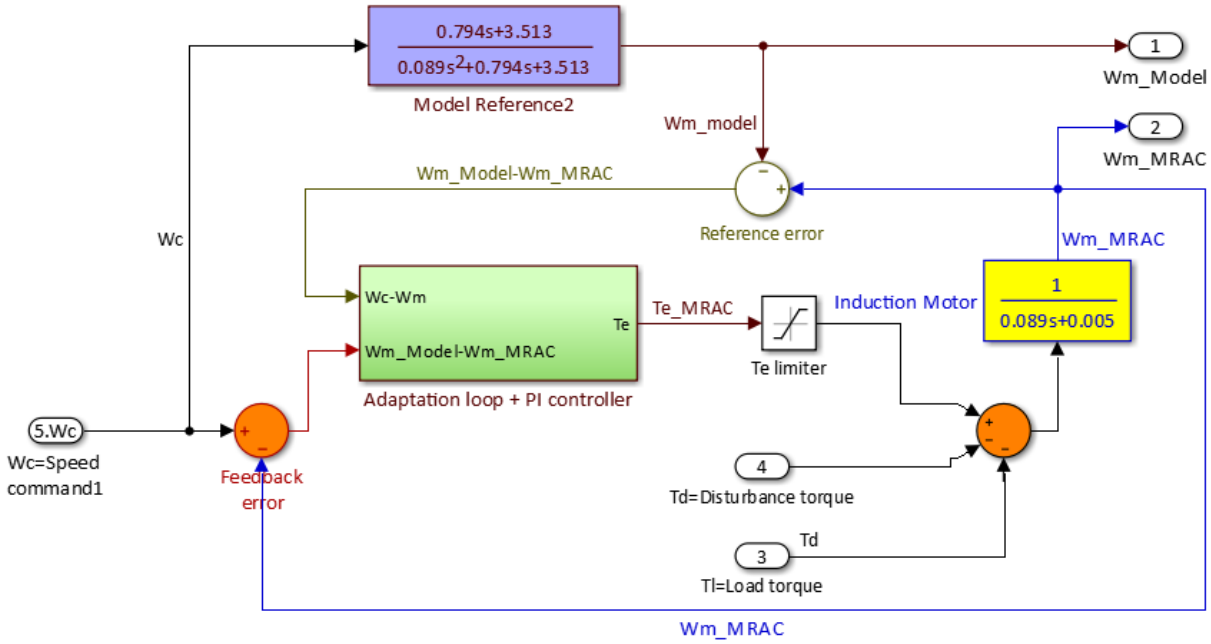

Figure 3.20 Simplified Design of Model Reference Adaptive Controller for AA-LRT Train

1. The demanded speed command signal (reference) will be given to reference model and feedback comparator
2. Feedback comparator compare the speed command and the actual motor speed, and it generates error signal, this error signal sent to PI adaptation loop.
3. The reference model will give required torque output based on the speed command, the output of the reference model with the actual plant output to generate error signal at reference error1 comparator. This error signal used as input for the Adaptation loop + controller block
4. In Adaptation loop plus controller block according to feedback error and reference error, controller gains will be corrected and adapted torque will be generated.
5. The output torque command of the Adaptation and control loop will be limited for operational issues like protecting the motor from over current. After the torque limiter Load torque and disturbance torque introduced and compared with generated electrical torque to achieve the target speed.

On MathLab Simulink the system response for different working conditions will be simulated and it will be discussed in the next chapter

Chapter Four

Simulation Result Analysis and Discussion

In this chapter, simulation of PI controller and MRAC controller is done using MathLab /Simulink environment. SIMULINK® is a toolbox extension of the MATHLAB program. To simulate dynamic systems responses, it is capable of performing complex dynamic system simulations, graphical environment with visual real time programming and broad selection of toolboxes. The toolbox is best in solving both linear and nonlinear processes, so it is perfectly suited to simulate braking responses.

For all simulations of this dissertation, the parameters used in this thesis are based on the actual data obtained from the ERC, approximate calculation and also some assumptions taken under different conditions.

Table 4.1 Parameters for Simulation

Parameters used for simulation		
Maximum operation speed:		70 km/h
Train Weight	Empty vehicle (tonne)	44
	Searing capacity (tonne)	59.24
	Overload capacity (tonne)	63.02
Axle load		≤11（1+3%）tonne
Maximum service brake deceleration		≥1.1m/s2 3.96 Kmphs
Supply voltage		DC 750V
Rated traction power:		2×130KW
Wheel diameter		Φ660mm (new wheel)/Φ580mm (full wear)
R=wheel radius		0.29 meter
D=gradient in 1000 m		54.2
R=curve radius		1200 meter
Gear ratio		8.2
Traction Motor	Rated power	130KW
	Synchronous Speed	190.5 rad/sec
	Rated torque	689N·m

First model of proportional and integral control which is developed in the previous chapter will be modeled in Simulink. Then the controller performance will be simulated under different conditions.

Then the proposed Model Reference Adaptive Controller will be simulated with the same procedure as the PI controller.

Finally the Existing Braking controller and the Proposed Braking controller will be employed to braking system model and simulated under different conditions, the result of each controllers will be discussed.

4.1 MathLab Simulation of Proportional and Integral Controller

PI controller model developed in chapter three (see Figure 3.17) is simulated on this section with different parameter conditions. Load rejection, braking transient and disturbance rejection capability are the major transient and steady state responses to be analyzed. The following sections discuss these major responses accordingly.

4.1.1 Load Rejection in PI Controller

Generally load rejection capacity in the controller is demonstrated by applying zero reference speed and constant loading torque. For this particular case speed command is 0 rad/sec, 665.9 Nm without disturbance, the demonstration takes 5 seconds. As Figure 4.1 depicts, there is 20% overshoot for the desired bandwidth depending the switching frequency of the inverter.

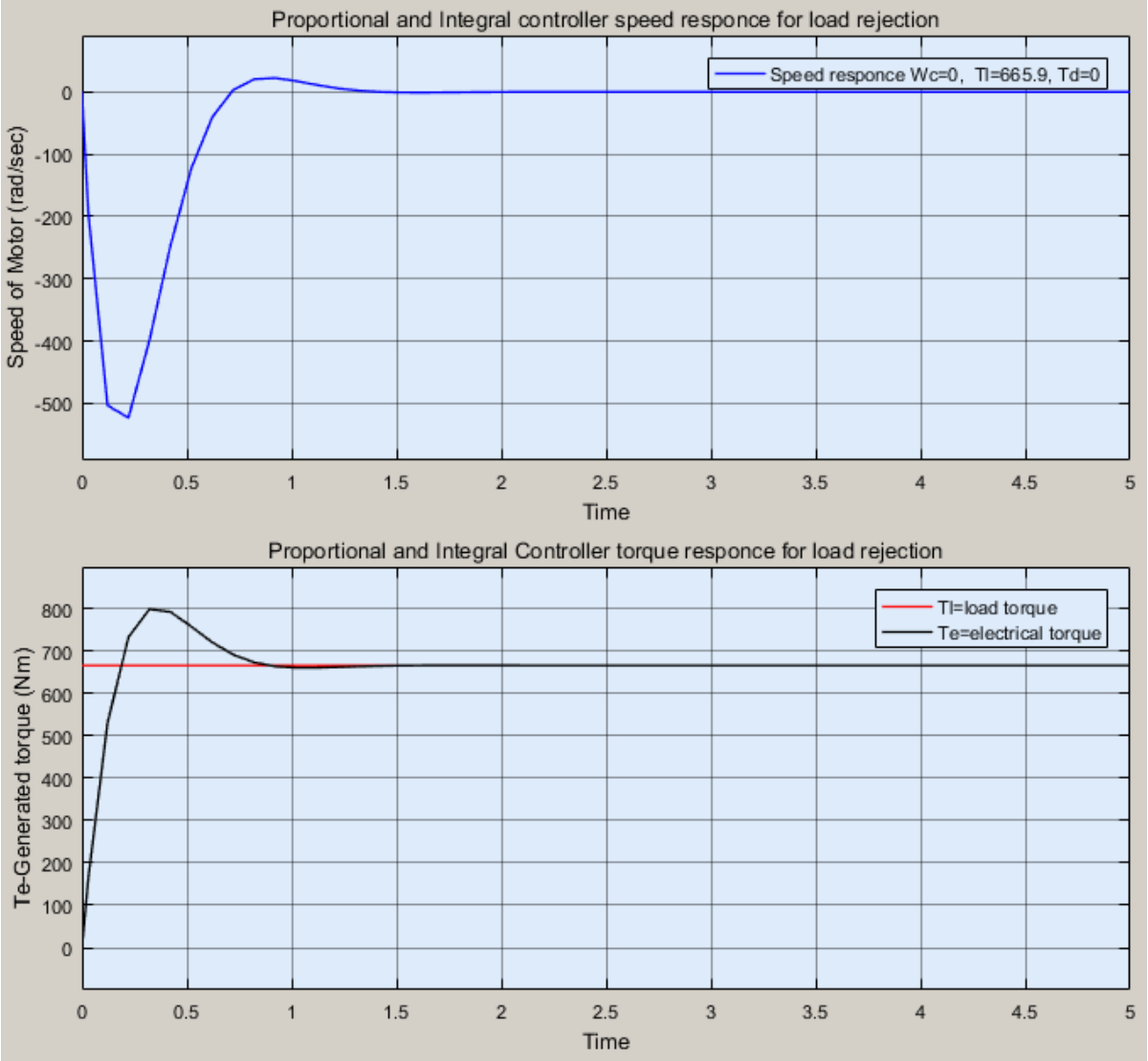

Figure 4.1 Load Rejection of PI Controller

4.1.2 Braking Transient Response of PI Controller

The command speed is applied in such a way that the train is traveling with its maximum allowable speed and going to stop after two seconds.

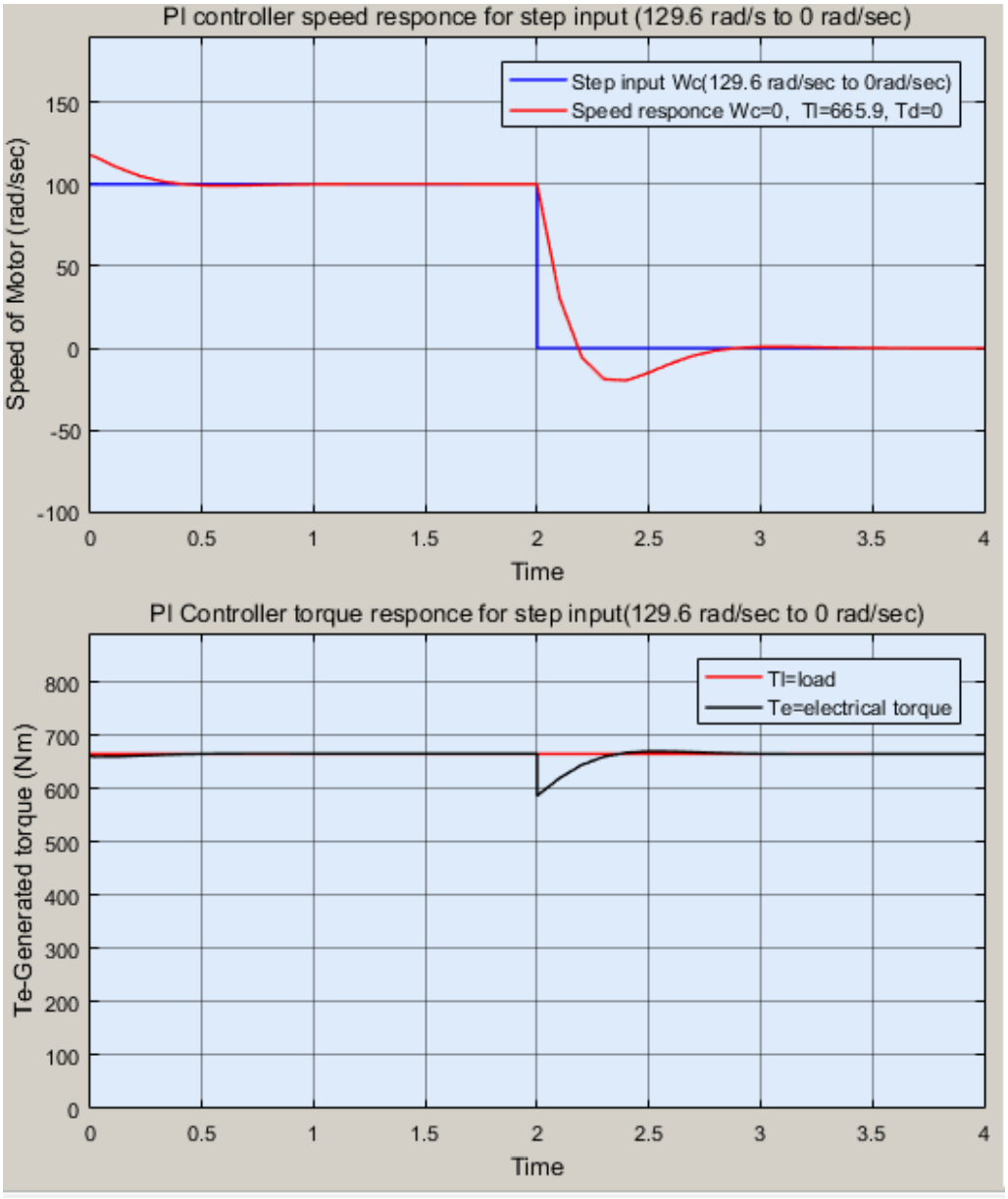

Figure 4.2 Braking Transient Response of PI Controller

Here the point of interest is how the speed and the traction torque behaves (not the starting characteristic.) Figure 4.1. Shows the speed and traction torque response of a train which traveled with 129.6 rad/sec for 2 seconds and came to stand still after all. The load torque is constant 665.9 Nm without any disturbance. As the wave shape implies, during braking the

speed has a negative overshoot due to the second order pole characteristic of closed loop transfer function, there is a negative overshoot for both and torque transients

4.1.3 Disturbance Rejection of PI Controller

With the same procedure like load rejection, step disturbance is added to the constant load torque with a value not more than10 % of nominal torque [35] i.e. - 60Nm for 2.1 sec and 60Nm afterwards. The PI controller could not reject the disturbance torque, instead it has contributed unstable condition by increasing the overshoot of the speed over 92.7% and it result average 6.26 rad/sec speed error (See Figure 4.3).

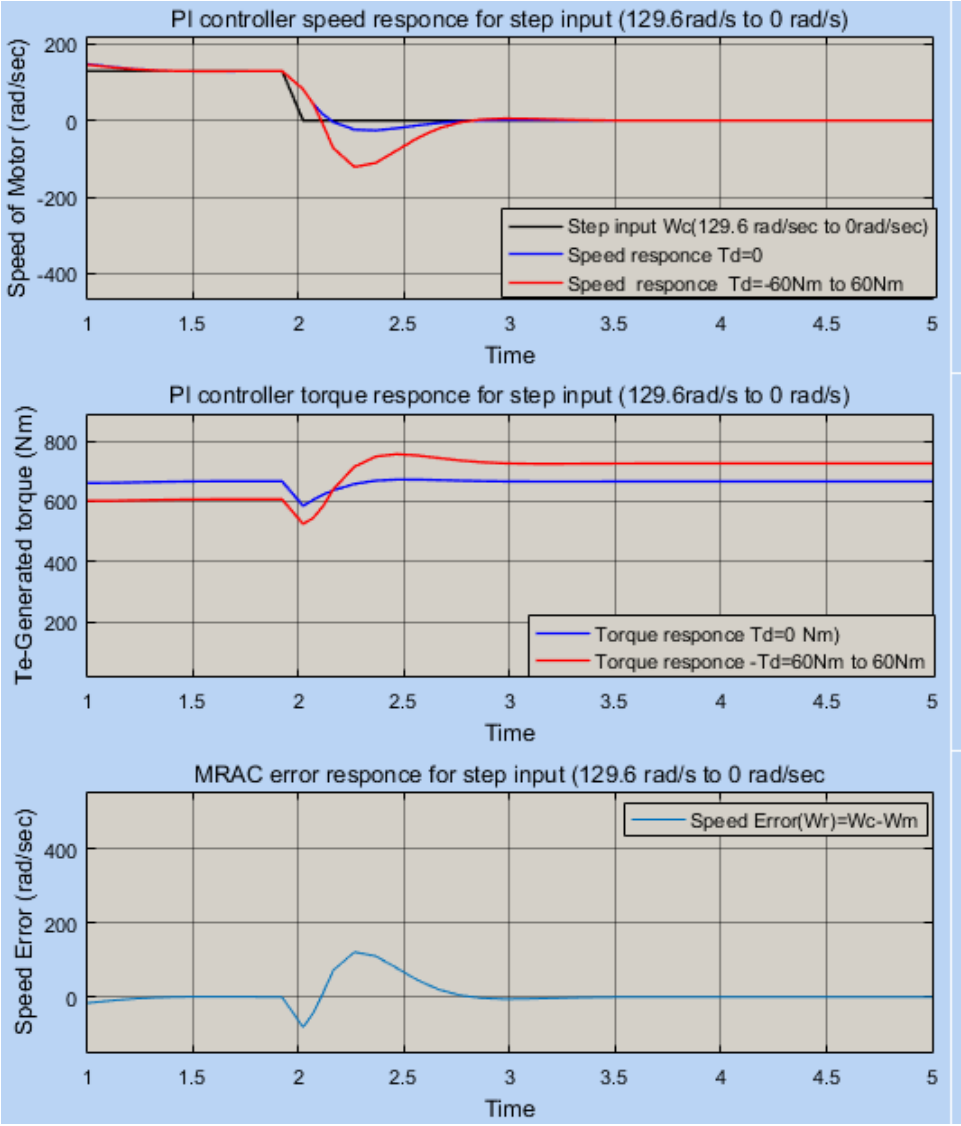

Figure 4.3 Disturbance Rejection of PI Controller

4.2 Model Reference Adaptive Controller

4.2.1 Load Rejection in MRAC Controller

Similar to the PI load rejection the MRA controller reject the load by varying adaptive gains as a controller parameter. At first cycle of the controller, the overshoot response of speed and torque is higher than its counterpart PI, however, it gets extremely reduced through adaptation (see Figure 4.4). In the figure it is clearly demonstrated how the MRAC adapt the process by varying γ_p (proportional) and γ_i(integral) adaptive gains.

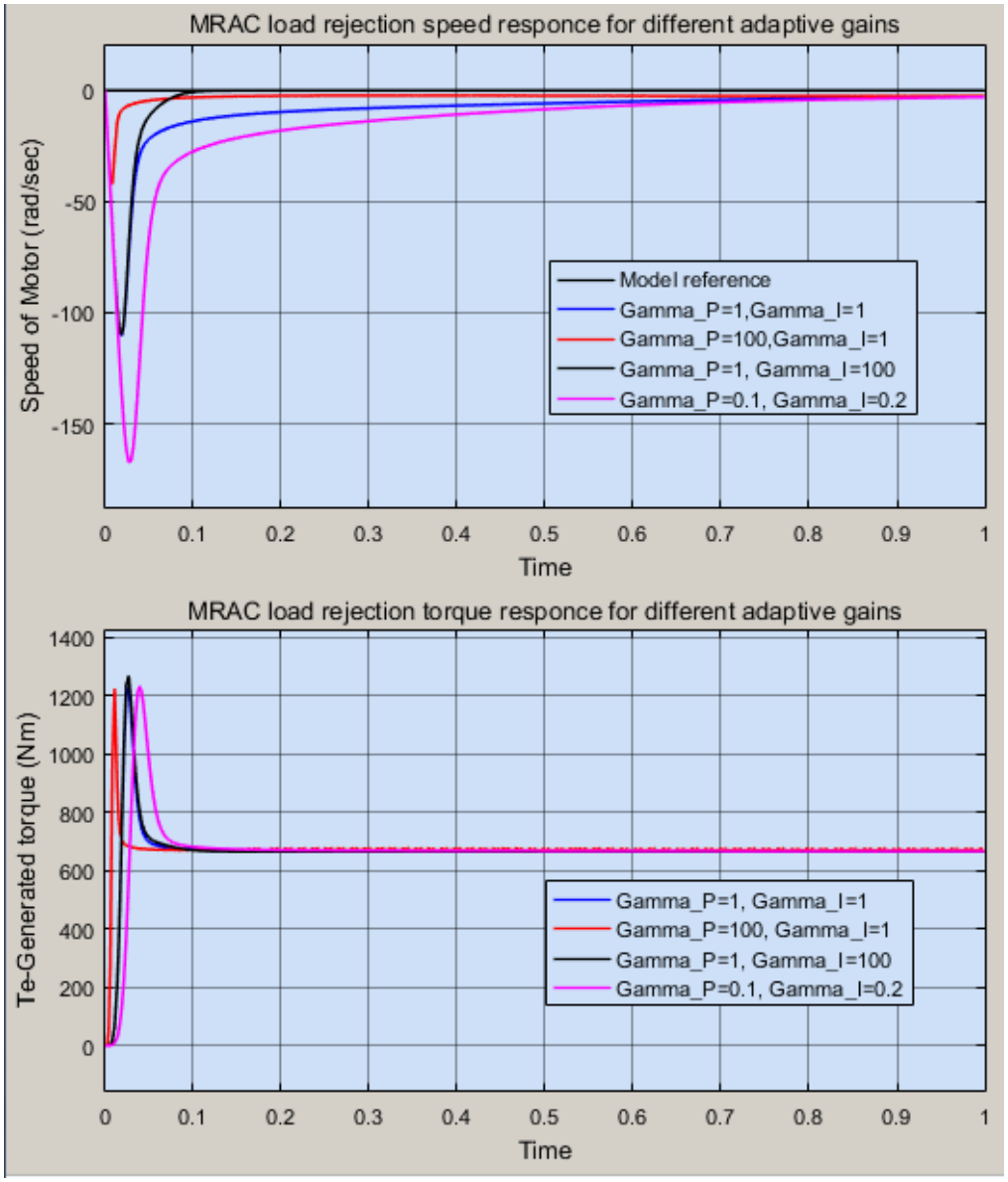

Figure 4.4 MRAC Controller Load Rejection for Different Adaptive Gain Values

4.2.2 Braking Transient Response of MRAC Controller

For the same parameters and sampling time applied to the MRAC controller, braking overshoot is avoided comparing with PI controller with significant difference with $\gamma_p = 1$ and $\gamma_i = 0.1$ Reference model response is looking like the PI controller response but MRAC adopted the difference between the reference model and actual plant response to achieve better response. It means that it can follow the step input from maximum speed to standstill as shown on Figure 4.5. Although the torque wave shape implies the torque impulse is too high, it is for very small micro seconds. Overall, the speed and torque response are smooth and robust for MRAC.

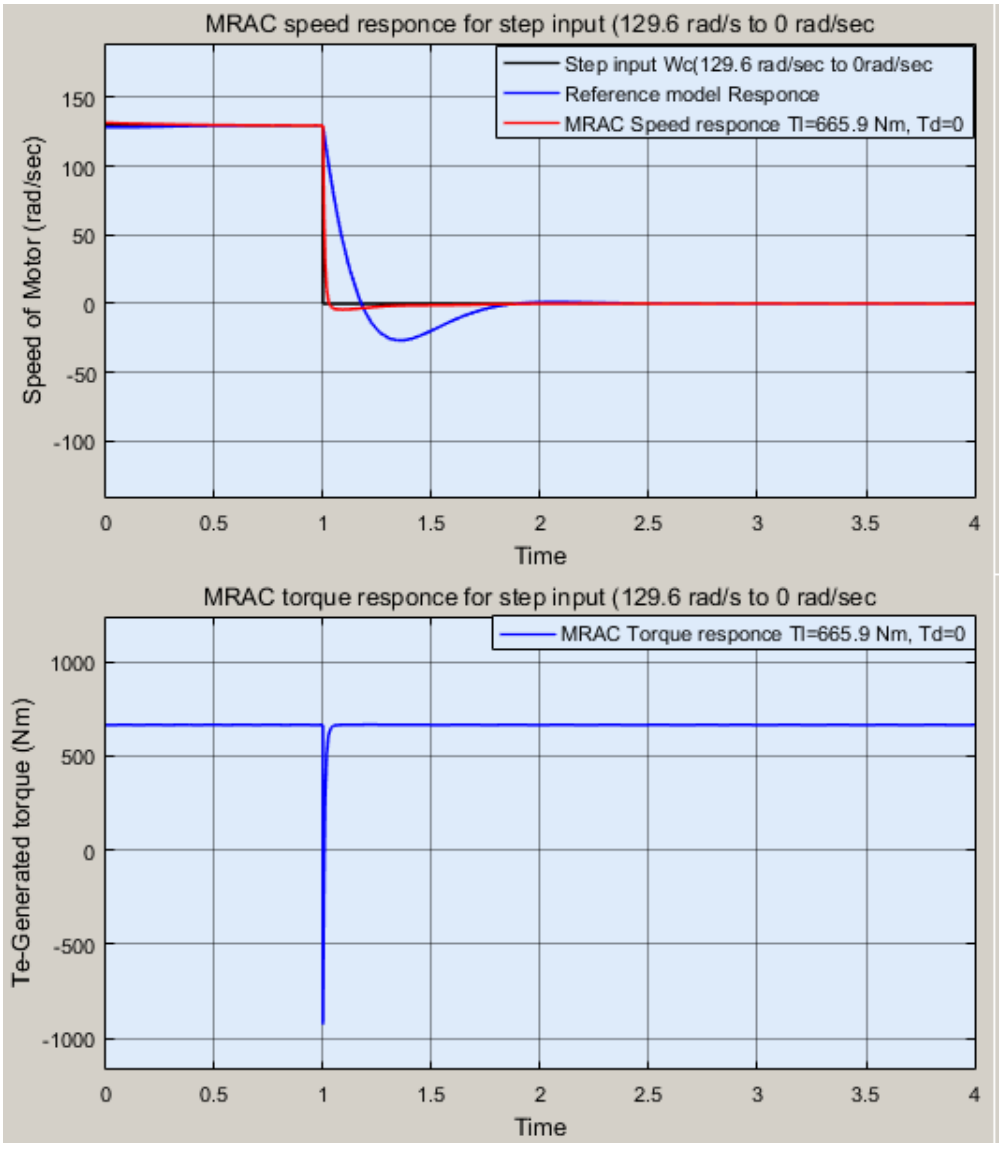

Figure 4.5 Braking Transient Response of MRAC Controller

4.2.3 Disturbance Rejection of MRAC Controller

The effect of MRAC is more visible on disturbance rejection which is frequently varying and prior indeterminate. As Figure 4.6 depicts, on the speed response graph there is no as such difference between the responses of MRAC controller due to absence and presence of disturbance torque. From Figure 4.6 it is observed that in the presence of disturbance MRAC controller result speed overshoot of 1.504 % and average speed error of 1.876 rad/sec.

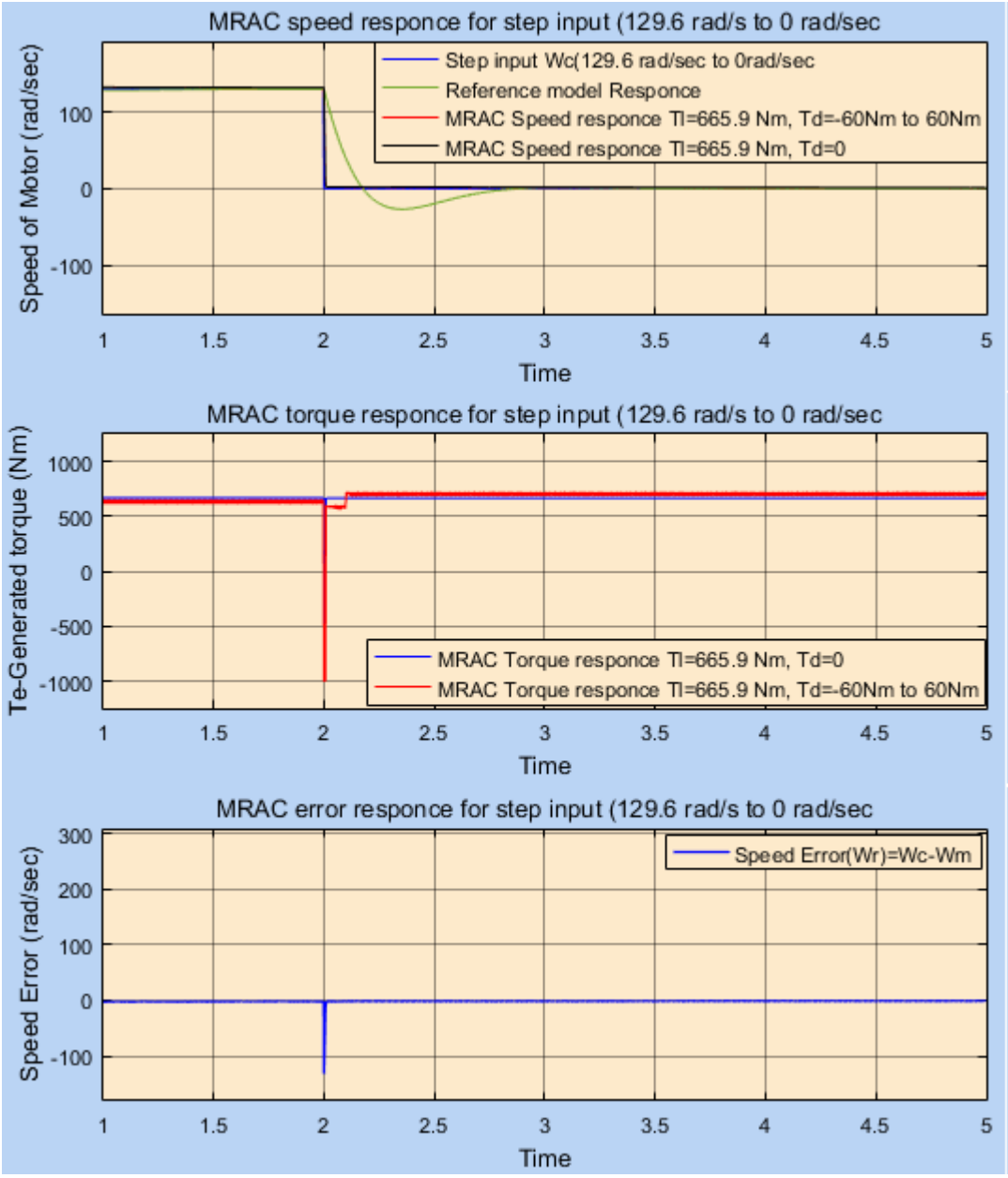

Figure 4.6 Disturbance Rejection of MRAC Controller

4.3 Performance of PI and MRAC Controllers in AA-LRT Braking System Model

In this section the two controllers will be integrated with braking model which is developed based on actual train parameters of AA-LRT. The complete model contains three main blocks as shown in Figure 4.7.

The first block is PI controller block, it contains PI controller as subsystem inside. It has three input ports for speed command, load torque and disturbance torque. On the output side there is one main port for braking torque output, this braking torque will be used as input for the braking plant. In addition it has output ports for displaying other values.

The second block is MRAC controller block, it is equipped with MRAC which is developed and demonstrated in the previous sections. The input and output configuration is the same with PI controller block.

The last main block is model of AA-LRT braking system, there two identical blocks to be used by the two controllers separately. In this block there are sub blocks to compute different forces, deceleration, braking time and distance. Train weight, speed and braking torque are the main inputs for this block. Braking time, braking distance, deceleration and load torque are the outputs of the block after some calculations. In this block and in its sub blocks train and track parameters can be defined easily. The following parameters are used for simulation, track parameters are for railway line between NS23 (Sebategna) - NS22 (Abinet) stations [5].

For adaptive controller the adaptations gains are $\gamma_p = 1$ and $\gamma_i = 0.1$

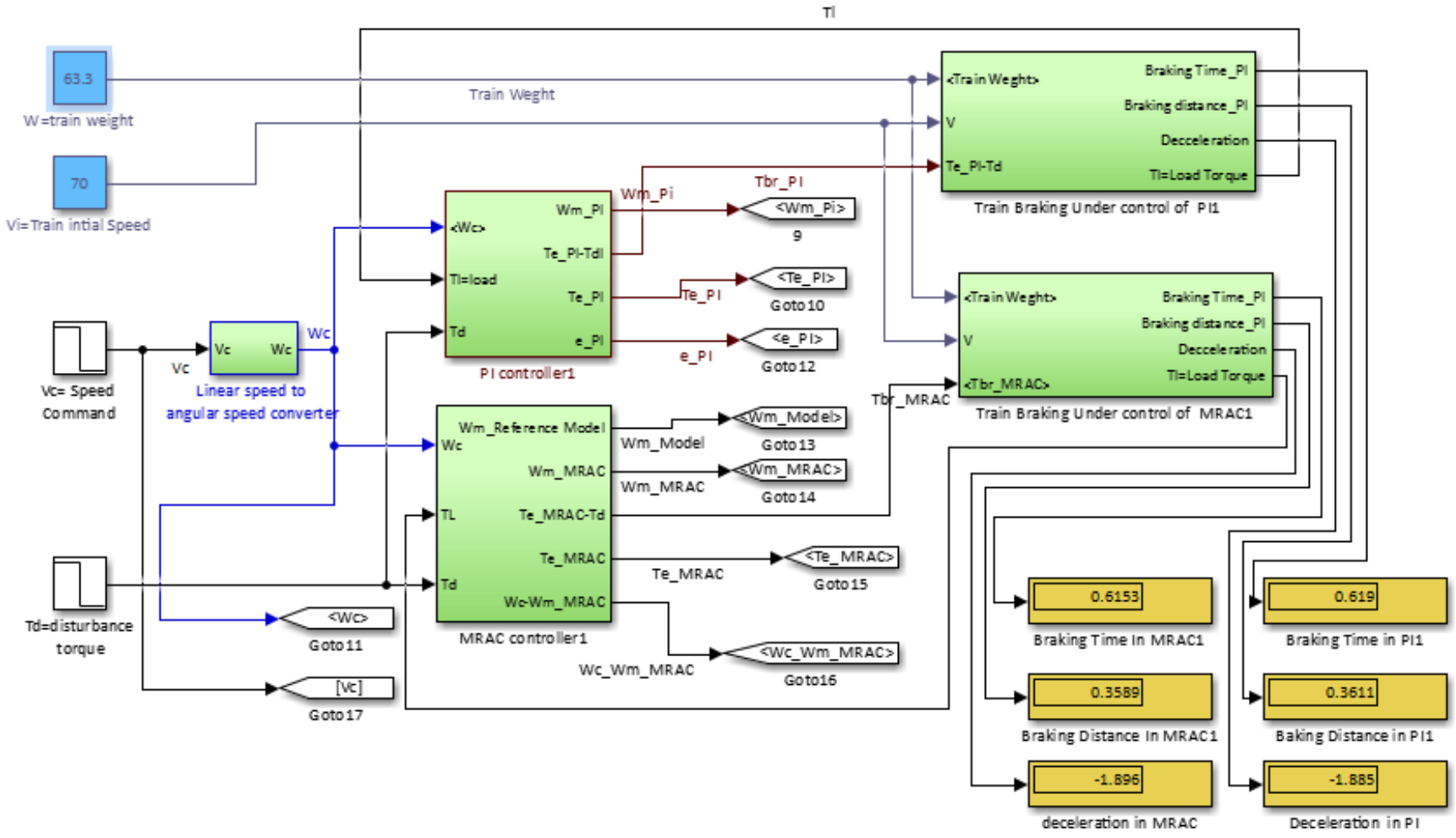

Figure 4.7 PI and MRAC Controllers in AA-LRT Braking System Compact MathLab Model

4.3.1 Simulation Results

Under Normal operation when braking is applied to bring the train from 70 Km/h to 0 Km/h, let assume step disturbance with 60KN introduced to the system 0.1 second after brake is applied. The velocity and angular speed response of the controllers is shown in Figure 4.8.

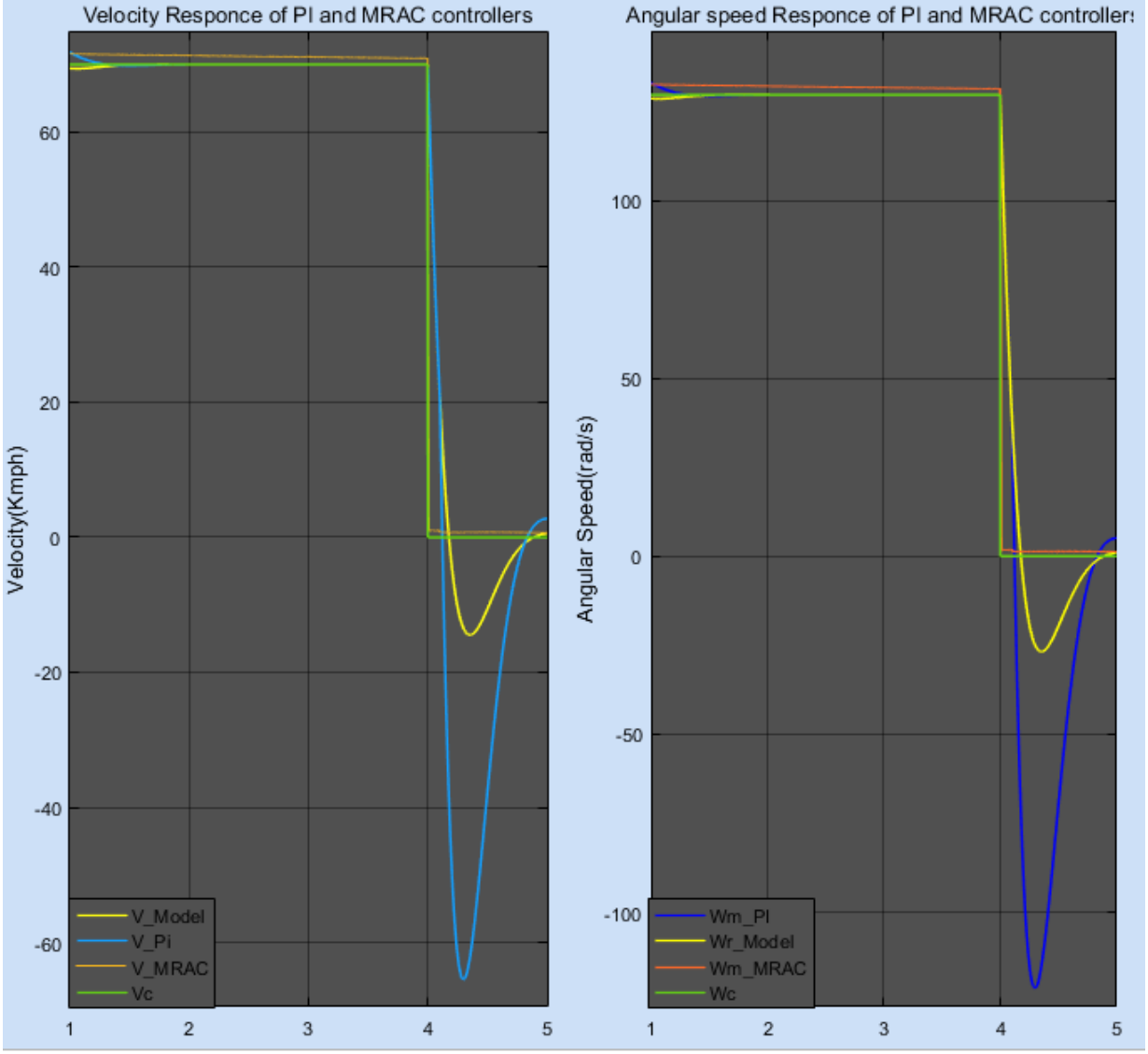

Figure 4.8 Speed Response of PI and MRAC Controllers in Braking Model.

From Figure 4.8 it is obsereved that MRAC controller is superiur over PI controller in the presence of diturbance. MRAC give an output reponce almost similar to the input command regardles of disturbance torque. But incase of PI controller when the disturbance occurs the system became unstable and creat high over shoot .

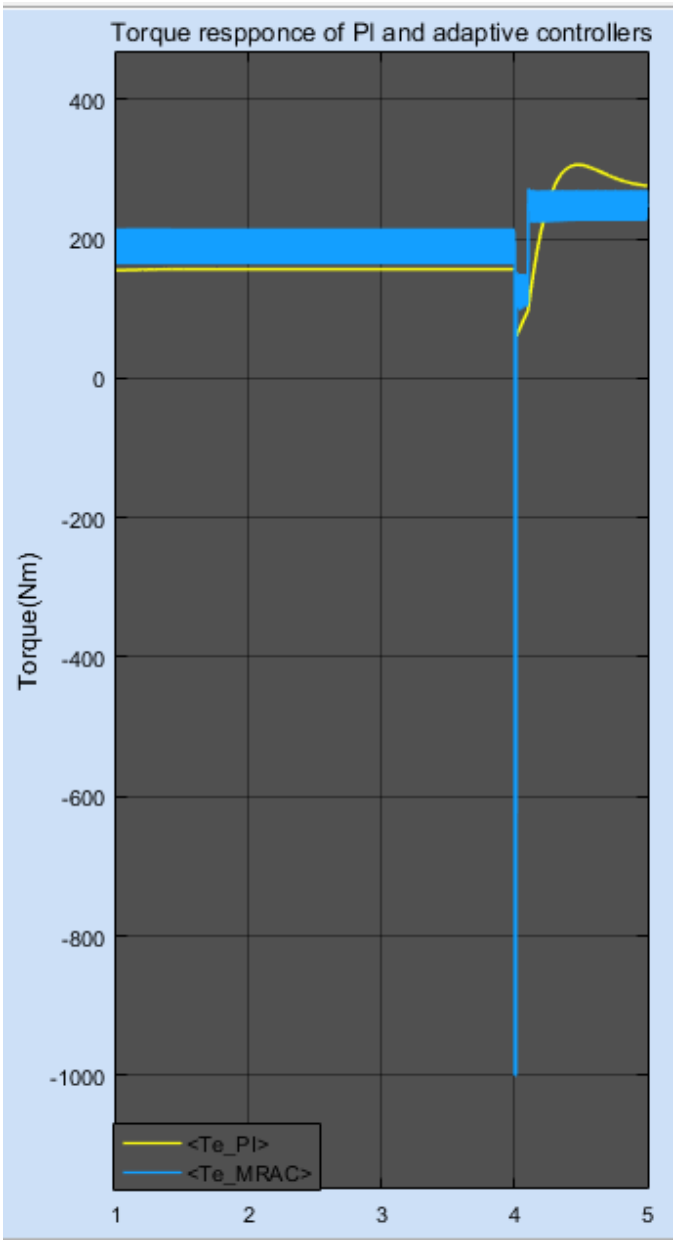

Figure 4.9 Torque and Deceleration Response of PI and MRAC Controllers

When brake is applied MRAC controller respond immidiatly generate maximum braking torque response (-1000 Nm) to reach maximum deceleration and to stop the train in short time and distance, incase of diturbance torque occure during the braking process MRAC controller will generate torque which will correct the error. Incase of PI controller the controller respond slowly and when disturbance occur the system became unstable.

The model demonstrated in case of different circumstances, the main outputs from the controler actions summarized in tabel as ashown bellow .

Table 4.2 Braking Performance of PI and MRAC

No.	Train weight (tonne)	Speed command (Km/hr.)	Disturbance torque (Nm)	Braking time (Minutes)		Braking distance (Km)		Deceleration (Kmphs)	
				PI	MRAC	PI	MRAC	PI	MRAC
1	63.3	70-0	60 Nm step signal	0.7433	0.7217	0.4336	0.421	-1.617	-1.57
2	63.3	70-0	60 Nm pulse signal	0.6183	0.5124	0.3607	0.2989	-1.887	-2.277
3	44	70-0	60 Nm pulse signal	0.619	0.4664	0.3611	0.2721	-1.885	-2.502
4	80	70-0	60 Nm pulse signal	0.618	0.5411	0.3605	0.3156	-1.888	-2.156
5	63.3	50-0	60 Nm pulse signal	0.6404	0.6373	0.2655	0.2668	-1.301	-1.308
6	63.3	20-0	60 Nm pulse signal	0.1872	0.1874	0.03119	0.03123	-1.779	-1.781
7	44	20-0	60 Nm pulse signal	0.1872	0.1874	0.0312	0.03123	-1.779	-1.781
8	63.3	70-0	10 Nm pulse signal	0.6162	0.6002	0.3595	0.3501	-1.893	-1.994

Table 4.3 Braking Performance Improvement in MRAC

Train weight (tonne)	Speed of train (Km/hr.)	Speed command (Km/hr.)	Disturbance torque (Nm)	Braking time distance improvement MRAC over PI controller
63.3	70	70-0	60 Nm step signal	3%
63.3	70	70-0	60 Nm pulse signal	17%
44	70	70-0	60 Nm pulse signal	25%
80	70	70-0	60 Nm pulse signal	12%
63.3	50	50-0	60 Nm pulse signal	0%
63.3	20	20-0	60 Nm pulse signal	0%
44	20	20-0	60 Nm pulse signal	0%
63.3	70	70-0	10 Nm pulse signal	3%

In Tables 4.2 and 4.3 PI controller and MRAC controller demonstrated in eight different cases

1. **Nomal working conditions with step disturbance(60Nm):** at normal load and maximum speed condtions MRAC not affected by the input diturbance and PI controller it affected slightly, improvement in braking distance/time achieved by MRAC is 3%.
2. **Nomal working conditions with pulse disturbance(Nm):** with the exstence of pulsating disturbance MRAC achive higher performance than PI controller, which is around 17%.
3. **Empty train and braking from maximum speed with pulse disturbance(60Nm):** MRAC reach highst deceleration point which is 2.502 Kmphs and improve braking performance by 25% than that of PI controller.
4. **Overloaded train and braking from maximum speed with pulse disturbance(60Nm):** Under over load conditions MRAC controller improve the performance 12 %.
5. **Normal load and slighty less speed (50Km/hr) with pulse disturbance(60Nm):** when the train operate less than the maximum speed both MRAC and PI controllers provide almost the same braking distance and time.
6. **Normal load and low speed (20Km/hr) with pulse disturbance(60Nm):** at low speed is PI controller give very small higer perfrmance than MRAC.
7. **Empty train and low speed (20Km/hr) with pulse disturbance(60Nm):** incase of the train is empty and operating at low speed braking will not be a problem, both controllers give same result.
8. **Nomal working conditions with pulse disturbance(10 Nm):** when disturbance with less magnitude introduced to the system MRAC is not affected and it achieved 3% improvement.

Chapter Five

Conclusion and Recommendation for Future Work

5.1 Conclusion

In this thesis, Addis Ababa LRT trams braking system, controller performance has been studied in detail and new controller type is developed to improve electrical braking performance. The main findings and results of the thesis can be concluded as follows.

Train braking is very complicated task since the process parameters changing every time and braking activity is mainly dependent on fast response. Controller is the brain of braking system which takes action in short period by considering the desired input and actual output.

From MathLab Simulink simulation results it is observed that PI controller has 92.7 % overshoot, 6.26 rad/sec speed error, it is unstable for a while and take control action slowly when there is disturbance in the system (see Figure 4.3). This have negative impact on the braking control action.

From Model Reference Adaptive Controller simulation in section 4.2.1 or Figure 4.4, the controller can be redesigned for different values controller adaptive gains, when proportional adaptive gain is higher than integral adaptive gain the controller can adapt the system easily. In Figure 4.6 it is observed that MRAC with $\gamma_p = 1$ and $\gamma_i = 0.1$ gains is not affected by 60Nm disturbance input and it give output with 1.504 % overshoot and 1.876 rad/sec speed error.

The simulation result from PI and MRAC controllers in MathLab model of AA-LRT braking system (see Figure 4.7), MRAC controller provide maximum of 25% higher reponce than PI controller in braking time and distance by handling different process diturbances as it is shown in Table 4.2 and 4.3.

Finally MRAC can adapt to changes in locomotive operating conditions, available braking effort, conditions in real time to provide better braking performance than non-adaptive controllers, such as PI control. MRAC allows the braking output to closely follow the designed reference model. Model Reference Adaptive Control (MRAC) can easily be implemented in locomotives to significantly improve electrical braking in terms of taking advantage of the maximum available braking from the traction motors, bringing the train to stand still in short time and short distance.

5.2 Recommendations

- Based on the result of this thesis that the existing VVVF drive controller is has some problems under torque disturbance it is recommended the application of other efficient controllers should be considered.
- In this thesis Model Reference Adaptive Controller based on MIT adaptation rule is used, to get optimum performance in adaptive controllers it is recommended to study the other adaptive controller types and adaptation rules.
- The thesis mainly investigates the performance braking control system using MATLAB/Simulink. It is better to use other software's or train simulators to see the dynamic nature of the traction load.
- In searching for related researches focused on AA-LRT it observed there are no such studies conducted in speed control and braking control, so it is highly recommended to work in this areas in the future.

References

[1]. Cătălin C, "Reliability and Safety in Railway", University POLITEHNICA of Bucharest, Bucharest Romania 2012.

[2]. Bin N,."Analysis of train braking accuracy and safe protection distance in automatic train protection (ATP) systems", Department of Communication and Control Engineering, Northern Jiaotong University, Beijing, China, 1996.

[3]. González-Gil, A., P. Roberto, and B. Paul. "Sustainable Urban Rail Systems: Strategies and Technologies for Optimal Management of Regenerative Braking Energy. Energy Conversion and Management, Vol. 75, 2013.

[4]. Husain A, "Dynamic Braking Control for Accurate Train Braking Distance Estimation under Different Operating Conditions, Doctoral Thesis", Virginia Polytechnic Institute and State University, Blacksburg, VA, USA, February, 2013.

[5]. China Railway Group (CRECG) Project Manager Office for Light Rail Project of Ethiopia, Technical Specifications of Vehicles, July 2013.

[6]. Garg, V. K., & Dukkipati, R. V. Dynamics of Railway Vehicle Systems. Ontario, Canada: Academic Press, 1984.

[7]. Manual for Railway Engineering, America Railway Engineering and Maintenance-of- Way Association (AREMA), Systems Management. Vol.4, 2010.

[8]. Shaofeng Lu, "Optimizing Power Management Strategies for Railway Traction Systems", Doctoral Thesis, University of Birmingham, October 2011..

[9]. Yirgalem H.,"Simulation of Electro-Pneumatic Braking System Response in Long Trains" Addis Ababa University Institute Of Technology School Of Mechanical And Industrial Engineering, Addis Ababa, Ethiopia, September 2014.

[10]. Daniel R., "Effect of Malfunctioning Of The Braking System On Thermo-Mechanical Properties Of Freight Train Wheels", Addis Ababa University Institute Of Technology School Of Mechanical And Industrial Engineering, Addis Ababa, Ethiopia, March 2015.

[11]. International union of railway, http://www.railway energy.org/static/Regenerative braking_ in_DC_systems_103.php, 2003

[12].Kibrom T. "Analysis of Regenerative Braking System in the Reduction of Energy Consumption in Addis Ababa light rail trains (LRT)", Addis Ababa University, Addis Ababa, 2014.

[13].Dieckerhoff, S. Bernet, D. Krug, "Evaluation of IGBT multilevel converters for transformerless traction applications", 34th IEEE Annual Power Electronics Specialist Conf., Vol. 4, pp. 1757-1763, June 2003.

[14]. M. Iordache, E. Mendes, C. Marchand, S. Belin, V. Mickiewicz, "Harmonic analysis method for traction drives EMI studies", IEE Proc. of Electrical Power Applications, Vol. 150, No. 4, pp. 431-438, July 2003.

[15]. M. Tulbure, R.Both, R. Festila," Analysis of the induction railway traction motor in regenerative braking",Technical University of Cluj-Napoca, Cluj-Napoca, Romania, pp. 26-28, 2012.

[16]. José A. Lozano, Jesús Félez, Juan de Dios Sanz and José M. Mera Universidad Politécnica de Madrid Spain

[17]. Landau et al., "Adaptive Control", Communications and Control Engineering, DOI, Springer-Verlag London Limited, 2011.

[18]. Petros A., Jing S., " Robust adaptive control", Prentice Hall, Upper Saddle River, New Jersey, 1996.

[19]. Priyank J., Nigam M.J, "Design of a Model Reference Adaptive Controller Using Modified MIT Rule for a Second Order System", Research India Publications, Uttarakhand, INDIA, 2013.

[20]. Jain S. Kumar, Nema R, "Comparative Analysis of MIT Rule and Lyapunov Rule in Model Reference Adaptive Control Scheme" Maulana Azad National Institute of Technology, Bhopal, INDIA, 2011.

[21]. China Railway Group (CRECG) Project Manager Office for Light Rail Project of Ethiopia,"Traction system specifications", July 2013.

[22]. CNR Dalian Electric Traction R&D Center Co., Ltd "CNE PW-260/D/H-02 Traction Converter User's Manual", May 2014.

[23]. Yongji Xinshisu Electric Equipment Co., Ltd "User's Manual for YJ128C Asynchronous Traction Motor"

[24]. Slobodan N. "Digital Control of Electrical Drives", University of Belgrade Faculty of Electrical Engineering, Bulevar Kralja Aleksandra, Serbia, 2007.

[25].Shilpa V., Prof. R.A.Keswani "Speed Control of Three Phase Induction Motor by V/f Method for Batching Motion System", Department of Electrical Engineering, Rashtra sant Tukdoji Maharaj NagpurUniversity, Nagpur, March 2013

[26]. Kharagpur, "Electrical Machine Drives module 7", EE IIT. 2005.

[27]. Devraj J., Nikhar Patel, "V/f Control Of Induction Motor Drive", Department of Electrical Engineering National Institute of Technology Rourkela, ODISHA, May 2013.

[28]. Aníbal T., Fernando J. "VSDs for Electric Motor Systems", ISR – University of Coimbra, London, England, 2010.

[29]. Prof. Krishna V., Prof. Sridhara R." Electrical Machines II', Indian Institute of Technology Madras, India, 2002.

[30].Chimurkar S., Tarnekar G. "Torque Control of Induction Machine Using V/F Method", Department of Electrical Engineering G. H. Raisoni College of engineering, Higna, Nagpur,2010.

[31]. Sweta S., "MATLAB Simulation for Speed Control of Three Phase Induction Motor Drive using V/F Control", Mesra, Ranchi, Jharkhand, India, 2016.

[32]. Smriti R., Ravi M." Comparative study of P, PI and PID controller for speed control of VSI-fed induction motor", Bhilai, Chhattisgarh, India, 2012.

[33]. MOHD N. "Three Phase Inverter For Induction Motor By Using Pi-Repetitive Controller", Faculty of Electrical and Electronic Engineering Universiti Tun Hussein Onn Malaysia, July 2014.

[34].Paul K, Oleg W, Scott S, Steven P." Analysis of Electric Machinery and Drive Systems", Institute of Electrical and Electronics Engineers, John Wiley & Sons, Inc., Hoboken, New Jersey, USA, 2013.

[35].Paul K, Oleg W, Scott S, Steven P." Analysis of Electric Machinery and Drive Systems", Institute of Electrical and Electronics Engineers, John Wiley & Sons, Inc., Hoboken, New Jersey, USA, 2013.

[36].Smarajit G. "Control systems theory and applications", Thapar university, pearson education, India, 2007.

[37]. R. Miller and M. R. Miller, "Electronics the Easy Way." USA: Barron's Educational Series Inc, 2002.

[38]. Devraj J., Nikhar Patel, "V/f Control Of Induction Motor Drive", Department of Electrical Engineering National Institute of Technology Rourkela, ODISHA, May 2013.

[39].Sung H., Jong S., Jeong J.," Modeling and Control of Adhesion Force in Railway Rolling Stocks", IEEE Control Systems Magazine, October 2008.

[40].Baljinder S. "Design and Simulation of Auto Tuning of PID Controller using MRAC Technique for Coupled Tanks System", Indian Institute of Technology, India,2013.

[41]. China Railway Group Limited "Preliminary Design for Ethiopia Addis Ababa E-W & S-N （Phase I） Light Rail Transit Project", 2012

Appendix

Appendix 1: MathLab code for plotting speed time curve in chapter 3 Figure 3.7

```
clear

deceleration1 =[0;0.360000000000000;0.771000000000000;0.943000000000000];

deceleration2 =[0;0.360000000000000;0.720000000000000;1.110000000000000];

deceleration3 =[0;0.360000000000000;0.630000000000000;1.210000000000000];

deceleration4 =[0;0.360000000000000;0.530000000000000;1.310000000000000];

speed= [0;70;70;0];

hold on;

grid on;

plot(deceleration1,speed,'Color','k','LineWidth',2.0);

plot(deceleration2,speed,'Color','R','LineWidth',2.0);

plot(deceleration3,speed,'Color','G','LineWidth',2.0);

plot(deceleration4,speed,'Color','B','LineWidth',2.0);

xlabel('Time(minutes)','Fontweight','Bold');

ylabel('Speed(km/hr)','Fontweight','Bold');

title ('Speed time curve for different deceleration values ','Fontweight','Bold');

legend ('3.96 km/hrs','3 km/hrs','2 km/hrs','1 km/hrs');

hold off;
```

Appendix 2: MathLab code for plotting Figure 3.12 Torque speed characteristics on 130 KW induction motor.

```
% M-file: torque_speed_curve.m
% First, initialize the values needed in this program.
w_sync = 190.5;          % Synchronous speed (rad/s)
r1 = 0.197;              % Stator resistance
l1= 0.00182;
x1 =w_sync*l1;           % Stator reactance
r2 = 0.164;              % Rotor resistance
l2= 0.00152;
x2 = w_sync*l2;          % Rotor reactance
lm= 0.001599;
xm = w_sync*lm;          % Magnetization branch reactance
v_phase = 500 / sqrt(3);    % Phase voltage
P=6;
n_sync = 1820;           % Synchronous speed (r/min)
% Calculate the Thevenin voltage and impedance from Equations
v_th = v_phase * ( xm / sqrt(r1^2 + (x1 + xm)^2) );
z_th = ((1i*xm) * (r1 + 1i*x1)) / (r1 + 1i*(x1 + xm));
r_th = real(z_th);
x_th = imag(z_th);

% Now calculate the torque-speed characteristic for many
% slips between 0 and 1.  Note that the first slip value
% is set to 0.001 instead of exactly 0 to avoid divide-
```

```
% by-zero problems.
s = (0:1:50) / 50;          % Slip
s(1) = 0.001;
nm = (1 - s) * n_sync;      % Mechanical speed

% Calculate torque for original rotor resistance
for ii = 1:51
  t_ind1(ii) = (3*(P/2) * v_th^2 * r2 / s(ii)) / ...
        (w_sync * ((r_th + r2/s(ii))^2 + (x_th + x2)^2) );
end

% Plot the torque-speed curve
plot(nm,t_ind1,'Color','k','LineWidth',2.0);
hold on;
xlabel('N-motor (RPM)','Fontweight','Bold');
ylabel('T-motor (Nm)','Fontweight','Bold');
title ('130 KW Induction Motor Torque-Speed Characteristic','Fontweight','Bold');
legend ('Original R_{1}');
grid on;
hold off;
```

Appendix 3

Adaptation and PI controllers sub block in Figure 3.20 Simplified design of Model Reference Adaptive Controller for AA-LRT Train.

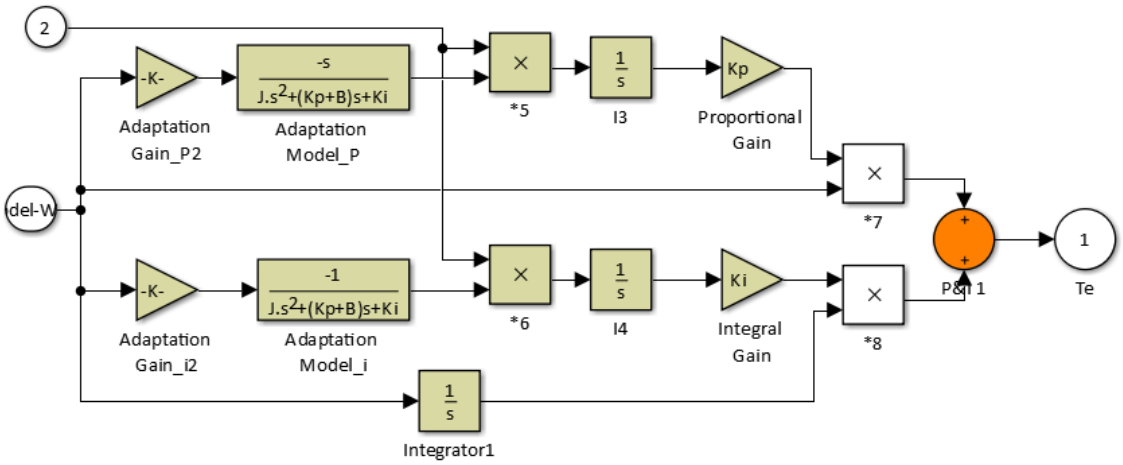

Appendix 4: Sub blocks in Figure 4.7 PI and MRAC controllers in AA-LRT braking system compact MathLab model.